

1 **Microbial assemblages on a cold-water coral mound at the SE Rockall Bank (NE Atlantic):**  
2 **interactions with hydrography and topography**

3

4 **J. D. L. van Bleijswijk<sup>1,\*</sup>, C. Whalen<sup>1,\*</sup>, G. C. A. Duineveld<sup>1</sup>, M. S. S. Lavaleye<sup>1</sup>, H. J. Witte<sup>1</sup>,**  
5 **and F. Mienis<sup>1</sup>**

6

7 <sup>1</sup>NIOZ Royal Netherlands Institute for Sea Research, P.O. Box 59, 1790 AB Den Burg,  
8 the Netherlands

9

10 \*These authors contributed equally to this work.

11

12 Correspondence to: F. Mienis ([fu.mienis@nioz.nl](mailto:fu.mienis@nioz.nl))

13

14 **Abstract**

15 This study characterizes the microbial community composition over Haas Mound, one of the  
16 most prominent cold-water coral mounds of the Logachev Mound Province (Rockall Bank, NE  
17 Atlantic). We outline patterns of distribution vertically--from the seafloor to the water column--and  
18 laterally--across the mound--and couple these to mound topography and hydrography. Samples of  
19 water, sediment and *Lophelia pertusa* were collected in 2012 and 2013 from locations that were  
20 chosen based on high definition video surveys. Temperature and current measurements were  
21 obtained at two sites at the summit and foot of Haas Mound to study near-bed hydrodynamic  
22 conditions. Overlaying water was collected from depths of 400 m as well as 5 and 10 m above the  
23 bottom using a CTD/Rosette system. Near-bottom water, sediment, and *L. pertusa* mucus and  
24 skeleton samples were obtained with a box-corer. Of all these biotopes, Roche GS-FLX amplicon  
25 sequencing targeting both Bacteria and Archaea was carried out, augmenting our understanding of  
26 deep sea microbial consortia. The pattern of similarities between samples, visualized by multi-  
27 dimensional scaling (MDS), indicates a strong link between the distribution of microbes and the  
28 specific biotopes. The microbial OTU diversity was highest in near-bottom water, which was sampled  
29 in the coral framework. For the first time, Thaumarchaeota MGI were found in *L. pertusa* mucus;  
30 *Ectoziocomonas* was detected in skeleton, mucus and near-bottom water; whereas *Mycoplasma* was  
31 only detected in skeleton and near-bottom water, however not in mucus. ANOSIM indicates that  
32 overlaying water is well-mixed at 400 m depth but less so at 5 and 10 m above the bottom, where  
33 the composition of microbial communities differed significantly between summit, slope and off-  
34 mound. At all locations, the near-bottom water differed significantly from water at 5 m above the  
35 bottom, illustrating that the near-bottom water in the framework represents a separate microbial  
36 habitat. The observed spatial heterogeneity in microbial communities is discussed in relation to  
37 environmental conditions.

38

39

## 40 **1 Introduction**

41 Numerous mounds composed of mixed sediment and cold-water coral debris line the Southeast  
42 slope of Rockall Bank between 500-1100 m water depth (Kenyon et al., 2003; van Weering et al.,  
43 2003). This so-called “Logachev Mound Province” consists of mounds varying from tens to hundreds  
44 of m in height and several km in length and width (Kenyon et al., 2003). These mounds have been  
45 developing since the middle Miocene-early Pliocene, largely as the by-product of interacting  
46 hydrodynamic regimes, coral growth and sedimentation (De Haas et al., 2009; Mienis et al., 2007).  
47 Living coral colonies of *Lophelia pertusa* and *Madrepora oculata* inhabit the mound summits and  
48 flanks, providing habitat for a wide range of invertebrates and fish (Costello et al., 2005; van Soest et  
49 al., 2008). Measurements of currents and temperature around the Logachev Mound Province have  
50 provided evidence of large regional differences with respect to current strength, temperature  
51 fluctuations, and organic carbon supply (Mienis et al., 2007). Significant heterogeneity in  
52 environmental conditions has also been found within individual mounds, such as between the  
53 summit and foot of mound structures (Duineveld et al., 2007). Recent studies on the near-bed  
54 hydrodynamic regime in the Logachev Mound Province revealed intense mixing on the mounds as a  
55 result of internal waves interacting with the topography (Mohn et al., 2014; van Haren et al., 2014).  
56 Such mixing provides a supply of food particles, i.e., phytodetritus, and constant refreshment of  
57 dissolved oxygen and nutrients (Findlay et al., 2014). The relevance of the hydrodynamic mixing  
58 regime for the growth of cold-water coral framework and mounds as a whole is a subject of current  
59 studies (F. Mienis, personal communication, 2014).

60 Other studies have already shown that cold-water coral reefs are hotspots of carbon mineralization  
61 (Rovelli et al., 2015; van Oevelen et al., 2009) and metazoan biodiversity and biomass (Biber et al.,  
62 2014; Henry and Roberts, 2007) and as such deserve our attention and protection. Whether these  
63 reefs are also biodiversity hotspots for microbial communities was qualified “questionable” based on  
64 low bacterial OTU numbers in ARISA profiles (Schöttner et al., 2012). Microbes are crucial for the  
65 fitness of tropical corals (Knowlton and Rohwer, 2003; Krediet et al., 2013; Rosenberg et al., 2007).

66 Shifts in the composition or metabolism of shallow-water coral-associated microbial consortia can  
67 significantly impair the health of tropical corals by increasing stress, the incidence and prevalence of  
68 disease, and causing mortality (Ainsworth et al., 2010; Dinsdale and Rohwer, 2011; Gilbert et al.,  
69 2012; Rohwer and Kelley, 2004).

70 In deep cold-water coral ecosystems insight into the distribution and variability of microbial  
71 communities is now also progressing. Research has begun to reveal patterns in the composition of  
72 microbial communities associated with cold-water corals (Emblem et al., 2012; Galkiewicz et al.,  
73 2011; Hansson et al., 2009; Kellogg et al., 2009; Neulinger et al., 2009; Neulinger et al., 2008; Penn et  
74 al., 2006; Schöttner et al., 2009; Schöttner et al., 2012; Yakimov et al., 2006) and the ambient  
75 environment (Jensen et al., 2012; Jensen et al., 2014; Jensen et al., 2008; Schöttner et al., 2012;  
76 Templer et al., 2011). On the basis of samples taken at a variety of spatial scales in relatively shallow  
77 cold-water coral reefs, Schöttner et al. (2012) concluded that bacteria in these CWC reefs are  
78 structured based on habitat (coral branch, mucus, water and sediment) and reef location (four reefs  
79 located off Norway). Archaea were not included in this study and water was sampled near the reef  
80 only, and not higher up in the water column. Adding to this, recently, Jensen et al. (2014) found  
81 highly similar bacterial communities in water sampled proximal (~1 m) and distal (30 m) to a reef,  
82 whereas in another reef proximal and distal water communities clearly differed.

83 In the present study a detailed analysis was made of the composition and distribution of microbial  
84 communities across Haas mound, a deep cold-water coral mound in the NE Atlantic. The main  
85 objective of this study is to provide insight into diversity of microbial communities (Bacteria and  
86 Archaea) within different biotopes at Haas Mound. Besides the water column these biotopes  
87 included the major surfaces that are in contact with the water, i.e., coral framework, coral mucus and  
88 sediment. Our hypotheses are 1) microbial communities, including Bacteria and Archaea, will be  
89 structured based on cold-water coral biotope; 2) the reef will have an effect on the microbial  
90 community composition of the associated water, and due to strong mixing, this effect will also be  
91 visible higher up in the water column, i.e., at 5 and 10 m above the bottom.

92

## 93 **2 Materials and methods**

### 94 **2.1 Location and sample collection**

95 Samples were collected during cruises 64PE360 (October 2012) and 64PE377 (October 2013) aboard  
96 the RV Pelagia (NIOZ) in the Logachev Mound Province on SE Rockall Bank (Fig. 1a). The focus site for  
97 this study was Haas Mound, one of the largest and highest carbonate mounds in the Logachev  
98 Mound Province (Mienis et al., 2006) (Fig. 1b). Two transects (Fig. 1c and Fig. 2), from the base to the  
99 summit of Haas Mound, were surveyed with a tethered HD video camera towed at 2 m above the  
100 bottom (mab). Videos were annotated on board and box-corer locations were selected representing  
101 the variation in coral cover and megafauna composition.

102 Microbial community samples (Table 1) were collected from a range of putative biotopes across Haas  
103 Mound that were operationally defined using video information, hydrographic data collected during  
104 the 2012–2013 cruises and earlier e.g. (Mienis et al., 2007), and literature on coral microbe  
105 interactions (Carlos et al., 2013; Kellogg et al., 2009; Schöttner et al., 2012; Wild et al., 2008). These  
106 biotopes were: (i) water well above the mound i.e. at 400 m water depth; (ii) water overlaying the  
107 coral framework at 5 and 10 mab; (iii) near-bottom water; (iv) sediment; (v) uneroded (recently  
108 deceased) and eroded *L. pertusa* skeleton; and (vi) *L. pertusa* mucus.

109 Box-core samples were taken with a 50 cm diameter, NIOZ designed box-corer. This box-corer is  
110 equipped with a tightly-sealing top valve that prevents the leakage and/or exchange of sea water  
111 overlaying the sample during ascent enabling sampling of the near-bottom water once the box-corer  
112 was on board. A total of 9 box-cores were collected on the two transects (Table 2, Fig. 1D and Fig. 2)  
113 and from these *L. pertusa* skeleton, mucus and near bottom water were taken when available. We  
114 differentiated between eroded and uneroded skeleton based on its discoloration (“white” for  
115 uneroded skeleton, without biofilm, and “brown” for eroded, older skeleton with biofilm). The water  
116 column overlaying Haas Mound was sampled using a rosette sampler equipped with 24 Niskin bottles  
117 of each 11 L, attached to a conductivity-temperature-depth (CTD) meter. For each CTD drop, water

118 was collected from three different depths: 1) 400 m, 2) 5 mab, and 3) 10 mab (Table 3, Fig. 1C and  
119 Fig.2). Also, one off-mound station at 1200 m water depth, situated 10 km SE from Haas mound was  
120 sampled with the CTD to determine if water mass characteristics near the mound differ from those  
121 off-mound and in deeper water.

122 Water sampled for microbial DNA analysis was filtered directly on 0.2 µm polycarbonate filters  
123 (Whatman) using mild under-pressure of 0.2 bar. From each water depth, 3 samples of 2 L were  
124 filtered from the same Niskin bottle. The near-bottom water collected from box-cores was sampled  
125 in a similar way (3 samples of 0,5 L were taken from the same box-core). Between two casts, the box  
126 corer was thoroughly cleaned and rinsed with seawater. All filters were immediately frozen in 6 mL  
127 Pony vials at -80 °C. Coral mucus as well as skeleton were sampled in at least three replicates  
128 (preferably from different colonies) following Schöttner et al. (2009). Except for skeleton in 2013,  
129 when we replaced the scraping technique described by Schöttner et al. (2009) by harvesting 0,5-1 cm  
130 of coral skeleton and directly freezing this at -80 °C on board. In the lab, these samples were exposed  
131 to liquid nitrogen and homogenized with sterile mortar and pestle.

132

## 133 **2.2 DNA Extraction and 16S rRNA amplicon sequencing**

134 DNA was extracted with Power Soil DNA Extraction Kits (MoBio) according to manufacturer's  
135 protocol and extracts were kept frozen at -20 °C. The concentration of the DNA in the extracts was  
136 measured with a F-2500 Fluorescence Spectrofluorometer (Hitachi, Tokyo, Japan) using QUANT-  
137 iT™PicoGreen® dsDNA kit (Life Technologies, USA). The quality was checked incidentally on a 1%  
138 agarose gel. To amplify the V4 region of the 16 S rDNA, the universal prokaryotic primer set S-DArch-  
139 0519-a-S-15 (5-CAGCMGCCGCGGTAA-3) (Wang et al., 2007) and S-D-Bact-0785-b-A-18 (5-  
140 TACNVGGGTATCTAATCC-3) (Claesson et al., 2009) were used as recommended in Klindworth et al.  
141 (2013). The forward primer was extended with a ten base molecular identifier (MID) barcode to  
142 distinguish the samples. Additionally the reverse primer also included a ten base barcode to  
143 distinguish the triplicates. To avoid PCR bias, per DNA extract, two separate 50 µL PCR reactions were

144 performed, using 1 unit Phusion Taq each (Thermo Scientific) in 1x High-Fidelity Phusion polymerase  
145 buffer. The volume of template material was adjusted according to the respective DNA concentration  
146 to aim for approximately 10 ng genomic DNA per reaction. The PCR was run on an iCycler™ Thermo  
147 Cycler (BioRad, USA). Cycle conditions were as follows: 30 s at 98 °C, then 30 cycles (10 s at 98 °C, 20  
148 s at 53 °C, 30 s at 72 °C), followed by 7 min at 72 °C. PCR products were loaded entirely on a 2% (by  
149 weight) agarose gel pre-stained with SybrSafe and run at 80 V for 50 min. Blue-light excitation was  
150 used when excising the PCR products to avoid UV-damage. Duplo PCR-products were pooled and  
151 purified using the Qiaquick Gel Extraction kit. After fluorimetric quantification as described above,  
152 equal amounts (70 ng) of the purified PCR-products were pooled (18 samples with their unique  
153 forward-MID and reverse- MID combination per set). Using a MinElute kit (Qiagen), the volume was  
154 adjusted to 25 µL with a final concentration of > 50 ng µL<sup>-1</sup> pooled PCR product per set. In total, 7 sets  
155 of samples were sent to Macrogen (Seoul, South Korea), each set sequenced using Roche GS-FLX  
156 instruments and Titanium chemistry on 1/8 region gasket.

157

### 158 **2.3 Sequence processing, taxonomic assignment and diversity analyses**

159 The sequence library of each sample set was filtered on length and quality, and sorted based on the  
160 forward MID using the Ribosomal Database Project (RDP) pipeline Initial process (Cole et al., 2014).  
161 Only sequences longer than 250 bases with average *Q*-score above 25 were kept. These sequences  
162 were reverse complemented and sorted according to the reverse MID tags into the 3 replicates. In  
163 both procedures only 2 mismatches in both primers and tags were accepted. At the end of the  
164 procedure, each of the seven libraries were split into 18 samples, 6 unique samples each with 3  
165 replicates. All reads had a similar length of 251 bp. Reads were aligned with PyNAST and checked for  
166 chimeras using ChimeraSlayer in Qiime. The read files were classified using the SILVAngs web  
167 interface (Yilmaz et al., 2014) with default settings (> 98% similarity of OTUs and > 93% classification  
168 similarity to closest relative in SILVA database 119).

169 OTU-tables were imported in PRIMERv6 (Clarke and Gorley, 2006). The number of reads per  
170 taxonomic unit was normalized per sample to avoid biases caused by differences in sample size.  
171 Methodological replicates (3 per unique sample) were pooled. Rarefaction curves and diversity  
172 indices were calculated using QIIME (Caporaso et al., 2010) and plotted in R. For a total of 40 samples  
173 (pooled from 121 independent methodological replicates: 38 triplo's and 2 duplo's namely water of  
174 400 m at station 36 and near-bottom water at station 72), the average number of reads per sample  
175 was 16678 (with standard error 1090). Rarefaction curves of OTUs plotted against reads per sample  
176 almost reached a plateau at 14000 reads per sample (S.I. Fig. 2 in the Supplement).

177 Differences in the microbial OTU composition were identified in PRIMERv6 (Clarke and PRIMER,  
178 2006; Clarke, 1993) by analysing Bray-Curtis distance for all pooled samples (n=40), and also for all  
179 methodological replicates (n=121). Results were visualized with MDS plots. DBRDA was done in  
180 PRIMERv6 on the samples taken at 5 and 10 mab with 7 variables (temperature, salinity,  
181 transmission, fluorescence, oxygen, Par and Spar) to explain the variability in microbial community  
182 composition within this sample group.

183 The OTU classification files were processed in Excel and class and genus data were selected for  
184 representation to allow easy comparison with other CWC studies (references mentioned in text).

185 The fractions of reads that were assigned to specific taxonomic units were 99% to class, 58% to  
186 family and 29% to genus level. Indicator OTUs, with significant non-random association ( $p < 0.0001$ ,  
187 9999 permutations) with one of the five biotopes, were identified with Indicator Species Analysis in R  
188 using the `indicspecies` package 1.6.7. (De Cáceres and Legendre, 2009) with display of both Indicator  
189 Values "A" and "B" (Dufrene and Legendre, 1997).

190

#### 191 **2.4 Near-bed temperature and current measurements**

192 During the 2012 cruise, temperature and currents were measured on the summit (st5 at 556 m) and  
193 at the foot of Haas Mound (st41 at 861 m) with an FSI™ 3DACM acoustic current meter (Falmouth



194 instruments) with temperature probe, which was attached to a benthic lander at 0.75 mab (Fig. 1c).  
195 The duration of each deployment was approximately 48 h.

196

## 197 **2.5 Data submission**

198 SSU rRNA gene amplicon pyrosequences are available via the NCBI Sequence Read Archive (number  
199 to be assigned upon publication).

200

## 201 **3 Results**

### 202 **3.1 Haas mound physical environment and coral cover**

203 The S-slope of Haas Mound is subject to strong daily variations in water mass properties due to  
204 internal tidal wave action causing deep, cold water to move up and down the slope (see details in  
205 van Haren et al., 2014). This results in a daily temperature fluctuation at the foot of the mound of 2.5  
206 °C as measured by the benthic lander. A much smaller temperature fluctuation i.e. less than 1 °C, was  
207 recorded on the summit (Fig. 3a). Temperature, salinity and oxygen profiles measured in 2012 and  
208 2013 are shown for the water column at the off-mound (st2 and 11), mound S-slope (st33), and  
209 mound summit (st12) of Haas Mound (Fig. 3b-d). The temperature of the water column overlaying  
210 Haas Mound was around 10 °C at 400 m depth and decreased by 1 °C with every additional 156 m  
211 depth. Salinity was 35.4 at 400 m depth and decreased slightly with depth. These temperature and  
212 salinity values are characteristic of Eastern North Atlantic Water. At the deeper off-mound st11  
213 temperatures decreased to 6.6 °C at 1000 m water depth (Fig. 3b), while salinity dropped to 35.2 (Fig.  
214 3c). Both values are indicative for the presence of Subarctic Intermediate Water (McGrath et al.,  
215 2012). The oxygen saturation was around 80% at 400 m depth. In the cold water at the far off-  
216 mound station (st2) oxygen saturation decreased at 1000 m to less than 70% after which an increase  
217 was observed at 1200 m to around 80% (Fig. 3d). Density of the water was 27.30 kg m<sup>-3</sup> at 400 m  
218 depth and gradually increased to 27.44 at 750 m, which is the depth of the slope of Haas Mound.  
219 Below 750 m, density increased to 27.60 where deep cold water was encountered. Bottom water

220 temperature at the far off-mound station (st2) was 5.3 °C, while salinity was 35.0 and density  
221 27.7 kg m<sup>-3</sup>.  
222 Video recordings along transects crossing Haas Mound showed large heterogeneity in coral  
223 framework distribution. The mound S-slope was characterized by dense framework while the mound  
224 summit showed reduced framework alternating with mud patches. At parts of the summit coral  
225 framework was replaced by a dense cover of large erect sponges (*Rosella nodastrella*). The foot of  
226 the mound S-slope (~645 m depth) was sampled by box-cores (st46), which revealed a thick layer of  
227 coral framework (Fig. 4B). Extensive coral framework was also sampled higher up the S-slope near  
228 the edge of the summit between 500-600 m depth (Figs. 2 and 4A). Density of the coral framework in  
229 box-core samples taken beyond the edge towards the central part of the summit contained reduced  
230 amounts of coral framework, which was in line with video recording (Figs. 2 and 4C,D). One box-core  
231 station (st24) yielded only mud and small fragments of coral skeleton (Fig. 4C).

232

### 233 **3.2 Microbial communities and diversity in Haas Mound samples**

234 The number of observed microbial OTUs (S.I. Table 1) was highest in near-bottom water (3858)  
235 followed by sediment (3245), skeleton (2856), mucus (2663) and overlaying water (1712).  
236 Corresponding Chao1 indices showed the same pattern, decreasing from 7876 in near-bottom water  
237 to 2684 in overlaying water. Initial MDS plot of the similarities in OTU composition of the samples  
238 immediately showed that the samples of the overlaying water taken at 5 and 10 mab did not differ.  
239 This was confirmed by ANOSIM ( $p > 0.1$ ; 999 permutations). Hence, these samples were pooled in  
240 one category indicated hereafter as 5 and 10 mab. Subsequent MDS plots were made of the  
241 similarities in the sample set and these revealed a consistent pattern, i.e. five different clusters which  
242 correspond with the biotopes of the samples (Fig. 5, S.I. Fig. 1). The same clusters were apparent in  
243 plots of microbial classes and genera. Overlaying water at 400 m grouped together with water at 5  
244 and 10 mab and formed a tight cluster (Fig. 5). Near-bottom water, which is closely associated with  
245 both reef and sediment, clustered distinct from overlaying water, sediment, *L. pertusa* skeleton and

246 *L. pertusa* mucus. Following is an account of the composition of the bacterial communities  
247 encountered in the samples with emphasis on variation between biotopes and within clusters  
248 (biotopes) across the mound.

249

### 250 **3.2.1 Variation between biotopes**

251 In near-bottom water, Gammaproteobacteria (22%) and Thaumarchaeota marine group I (22%) were  
252 the most abundant classes followed by Deltaproteobacteria (11%) and Alphaproteobacteria (9%).

253 Other biotopes shared these 4 groups, however with different relative abundances (Fig. 6A).

254 Sediment and overlaying water both contained relatively less Gammaproteobacteria (14% in  
255 sediment; 18% in overlaying water) and more Thaumarchaeota MGI (24% in sediment; 31% in  
256 overlaying water) than near-bottom water. *L. pertusa* skeleton and mucus contained lower relative  
257 amounts of Thaumarchaeota MGI (9% and 11% respectively) than near-bottom water but still a  
258 substantial percentage of their total microbial communities.

259 Mucus was very rich in Gammaproteobacteria (49%) and also Flavobacteria (4.1%) whereas

260 Betaproteobacteria (2.9%) were relatively high compared to other biotopes. Near-bottom water  
261 contained relatively high amounts of Halobacteria (1.2%) compared to other biotopes (<0.7%).

262 Sediment contained a higher percentage of Acidobacteria (6.0%) compared to other biotopes (<4.2%)

263 whereas skeleton was relatively rich in Acidimicrobiia (5.4%) and Planctomycetia (5.6%) compared to  
264 other biotopes (<2.9%, and <3.5% respectively). In overlaying water we found relatively high

265 amounts of Deferribacteres (5.9%) and Thermoplasmata (6.1%) compared to other biotopes (<2%).

266 Plotting the relatively most abundant genera (i.e., > 0.5% of all reads) confirmed a distinct signature

267 of near-bottom water (Fig. 6B) with a top 6 of *Nitrosopumilus* (3.2%), uncultured Xanthomonadales

268 (1.6%), *Defluviicoccus* (1.3%), *Marinicella* (1.2%), *Nitrosococcus* (0.8%) and the Brocadiaceae W4

269 lineage (1.1%) and a higher relative amount of *Colwellia* (0.6%) compared to the other biotopes (<

270 0.1%).

271 Overlaying water was relatively rich in Salinisphaeraceae ZD0417 marine group (1.9%) and  
272 Rhodospirillaceae AEGEAN-169 marine group (2,0%) compared to other biotopes (<0,4% and <0.3%  
273 respectively). *Pseudospirillum*, *Nitrosopumilus*, *Nitrospina* and the Flavobacteriaceae NS5 group each  
274 contributed between 0.5 and 1.1% to the microbial community of the overlaying water. A  
275 comparison of the relative abundance of the class Thaumarchaeota MGI with the abundance of the  
276 genus *Nitrosopumilus* indicates that the latter contributed ~2.5% to this class in overlaying water  
277 (~17% in near-bottom water and sediment, and ~35% in skeleton and mucus), meaning that other,  
278 unknown genera contributed 97% to the Thaumarchaeota class in overlaying water.

279 Sediment was relatively rich in uncult. Xanthomonadales (2.9%) and *Nitrosococcus* (1,5%) compared  
280 to other biotopes (< 1.7% and >0.8% respectively ), whereas skeleton samples contained relatively  
281 high percentages (>1%) of *Nitrosomonas*, *Nitrospira*, *Entheonella*, *Granulosicoccus*, *Rhodobium*,  
282 *Blastopirellula* and *Pseudahrensia*, compared to other biotopes (<0,5%). Mucus samples contained  
283 large amounts of Alteromonadaceae BD1-7 clade (22%, SE 9%) and *Acinetobacter* (9%, SE 9%), with  
284 high variability between the samples. *Endozoicomonas* (1.5%), *Polaribacter* (1.3%), *Pseudomonas*  
285 (1.0%) and *Aquabacterium* (1.9%) were also outstanding in mucus compared to other biotopes.  
286 *Mycoplasma* was not found in mucus but this genus was present in low percentages in skeleton  
287 (0.03%) and near-bottom water (0.01%).

288 Specific indicators, i.e. taxa that showed a significant non-random association to a specific biotope,  
289 were found for all biotopes (S.I. Table 1 in the Supplement). The number of strong indicators (i.e.,  
290 given the indicator is present, the probability that the sample belongs to a certain biotope > 0.85)  
291 was highest in near-bottom water and mucus (8 and 12 strong indicators, respectively) and low in  
292 overlaying water, sediment and skeleton (4, 0, and 0 strong indicators, respectively). Brocadiaceae  
293 W4, and Dehalococcoidia were the most abundant strong indicators in near-bottom water whereas  
294 SAR11 clade Deep 1 and Oceanospirillales ZD0405 were typical for overlaying water. Mucus was  
295 characterized by Alteromonadaceae BD1-7 and *Acinetobacter*.

296

### 297 3.2.2 Variation within biotopes

298 Within clusters belonging to two of the five main biotopes, patterns were present that could be  
299 related to additional factors (Fig. 8 and 9). Within the overlaying water cluster, depth category (400  
300 versus 5 and 10 mab) and year (2012 versus 2013) were discriminating factors as illustrated in the  
301 MDS plot (Fig. 8) and determined by ANOSIM ( $p < 0.01$  and  $p < 0.0001$ , respectively, 9999  
302 permutations). Samples taken at 400 m differed significantly from samples taken at 5 and 10 mab.  
303 Within this latter group, three clusters were recognized according to their geographic position.  
304 Samples taken on Haas Mound summit (st12, 36, 10 and 15) clearly differed ( $p < 0.001$ , 9999  
305 permutations) from samples taken at deeper locations on Haas Mound slope (st33 and 13) and from  
306 samples taken off Haas Mound (st2 and 11). Deeper samples contained relatively more  
307 Thaumarchaeota Marine Group I (Fig. 7A). Opposite trends (decreasing with depth) were detected in  
308 the classes Gammaproteobacteria, Alphaproteobacteria and Acidimicrobiia (Fig. 7A) and in the  
309 genera *Pseudospirillum*, *Nitrospina*, and *NS5 marine group* (Fig. 7B). A small but significant inter  
310 annual effect was present in the water samples taken at 400 m and at 5 and 10 mab on Haas Mound  
311 but not in samples taken off mound at 5 and 10 mab (Fig. 8). Distance based Redundancy Analyses  
312 indicated that depth correlated variables, i.e. temperature, salinity and density, only explained 17%  
313 of the total variation in microbial community composition of overlaying water at 5 and 10 mab.  
314 Turbidity of the water explained an additional 14% and was correlated with year ( $r=-0.97$ ).  
315 Within the cluster of skeleton samples, uneroded dead coral skeleton hosted a distinct microbial  
316 community from eroded dead skeleton (Fig. 9). Uneroded dead skeleton contained more of the  
317 classes Gammaproteobacteria and Sphingobacteria (Fig. 7C) whereas eroded skeleton communities  
318 contained relatively more Acidobacteria and Planctomycetia (Fig. 7C). On genus level, uneroded dead  
319 skeleton contained more *Nitrosopumilus*, *uncult. Xanthomonadales*, *Blastopirellula* and  
320 *Pseudahrensia among others*, whereas eroded skeleton contained more *Rhodopirellula*, Pir 4 lineage  
321 and *Rhodobium* (Fig. 7D). No patterns were found within the clusters of near-bottom water,  
322 sediment and *L. pertusa* mucus samples.

323

## 324 **4 Discussion**

### 325 **4.1 Microbial communities and hydrography**

326 The temperature measurements made during this study on Haas Mound support previous  
327 observations and models, showing that the S-slope of Haas Mound is subject to intensified mixing  
328 caused by internal waves (Mohn et al., 2014; van Haren et al., 2014). By contrast, conditions on the  
329 summit of the mound are less dynamic because the internal wave height is less than the mound  
330 height and the deep cold water does not reach the summit, but flushes around the slopes of the  
331 mound (van Haren et al., 2014). The distribution of dense, live coral framework on the slope seems  
332 to match with the degree of mixing, as framework was found to be less abundant on the summit  
333 (Figs. 2 and 4). This pattern suggests that mixing is important, for supplying food particles, i.e.,  
334 phytodetritus (Duineveld et al., 2007), to the living corals, as well as transporting dissolved nutrients,  
335 organic carbon, CO<sub>2</sub> and O<sub>2</sub>, as is observed near tropical shallow water reefs (Genin et al., 2002;  
336 Reidenbach et al., 2006).

337 The distribution of microbial communities across Haas Mound, in some aspects, also reflects local  
338 hydrodynamic patterns, though small inter annual effects are apparent. Microbial communities in  
339 the overlaying water at 400 m depth within a given year were very similar to each other. This result is  
340 explicable since this depth is well above the direct influence of the mound and absolute distances  
341 between successive CTD samples were small (< 1 km). Samples on- and off mound showed similar  
342 microbial compositions at 400 m. In contrast, samples at 5 and 10 mab differed between mound  
343 summit, mound slope and (deeper) off mound locations (Fig. 8). To explain this differentiation of the  
344 microbial communities according to mound location we infer that a gradient in environmental  
345 conditions exists on the mound. This hypothetical gradient is caused by internal waves coming from  
346 the deep and causing cold water to slosh up the slope, exposing the lower part to more intense  
347 mixing, lower temperatures and different water chemistry for longer periods than the upper slope  
348 while the summit is not reached by the wave (van Haren et al., 2014).

349 Microbial OTU diversity was highest in near-bottom water and decreased subsequently in sediment,  
350 skeleton, mucus and overlaying water. Likewise (Schöttner et al., 2009) found highest microbial OTU  
351 diversity in sediments followed by overlaying seawater, mucus and skeleton in a Norwegian cold  
352 water coral reef. Possibly the enhanced microbial diversity of near-bottom water also reflects the  
353 enhanced biodiversity of metazoans living on the coral framework (Bongiorni et al., 2010).

354 Due to our method of collecting near-bottom water within the framework with a box-corer,  
355 a certain amount of suspended sediment could be expected in the near-bottom water sample and  
356 indeed in the MDS plot (Fig. 5) the cluster of near-bottom water is situated in between the clusters of  
357 overlaying water and sediment. However, from the inventory of microbial classes present in the  
358 biotopes it is apparent that near-bottom water supports a microbial community clearly different  
359 from a mixture of overlaying water and sediment. Moreover, near-bottom water contained a number  
360 of strong indicator taxa that were highly specific (high A values in indicpecies analyses) for this  
361 biotope confirming its distinct signature (S.I. Table 2).

362 The large difference between near-bottom water and overlaying water at 5 and 10 mab was not  
363 anticipated given the strong turbulent mixing in places. We hypothesize that this difference is due to  
364 the effect of the dense 3-D coral framework constraining the exchange between the near-bottom  
365 water in between the coral branches and the water overlaying the reef. As a consequence of  
366 prolonged residence time and close contact with the dense epifauna (e.g. sponges, bivalves,  
367 foraminifera, crinoids) living in the framework and sediment, a biologically and chemically unique  
368 and sheltered environment is created for the development of a typical local microbial community  
369 with a high diversity (this study). In contrast, Schöttner et al (2012) found low bacterial diversities in  
370 water sampled close to four Norwegian reefs. Also in contrast to our findings, Jensen et al. (2014)  
371 found very similar bacterial OTU compositions in water proximal (~1 m) and distal (30 m) to one reef.  
372 However, at another reef, these authors found differences between proximal and distal water  
373 samples, comparable to the differences we found between near-bottom water and overlaying water  
374 at 5 and 10 mab: i.e. less Alphaproteobacteria and more Gammaproteobacteria and Planctomycetia

375 in near-bottom water compared to overlaying water. We anticipate that samples taken at 1 m above  
376 the reef not always (depending on the hydrodynamic conditions) reflect the typical microbial  
377 community living in between the coral framework and that sampling water from between the  
378 framework is preferred.

379

#### 380 **4.2 Microbial communities associated with *Lophelia pertusa* skeleton and mucus**

381 Distinct communities were identified on dead coral skeleton and in freshly produced mucus of living  
382 coral. Skeleton and mucus contained a substantial amount of Thaumarchaeota Marine Group 1 (9%  
383 and 11 %, respectively) of which the majority was unclassified, and the genus *Nitrosopumilus* made  
384 up 3% in both sample types and *Cenarchaeum* 0.4% in skeleton and 0.1% in mucus. In addition, we  
385 found small amounts of the Euryarchaeota class Halobacteria (0.1% in skeleton and 0.3% in mucus)  
386 and in mucus also Thermoplasmata (0.2%). It is for the first time that Archaea are detected in coral  
387 mucus. Archaea had been reported already (Emblem et al., 2012) in samples of *L. pertusa* tissue with  
388 corallites crushed, and with Archaea affiliated to three species prominently present in the top-10 of  
389 prokaryotic species based on 454 read data: *Nitrosopumilus maritimus*, *Cenarchaeum symbiosum*  
390 and *Candidatus Nitrosoarchaeum* sp..

391 Although not detected by Yakimov (2006), two bacterial genera were previously reported to be part  
392 of the *L. pertusa* biome, *Mycoplasma* and TM7 (Kellogg et al., 2009; Neulinger et al., 2009; Neulinger  
393 et al., 2008). In this study, using 454 sequencing, we detected these genera in low relative amounts:  
394 *Mycoplasma* was detected in skeleton (0.028%), near-bottom water (0.013%) and overlaying water  
395 (0.001%), however not in mucus and sediment. Candidate division TM7 was found in all biotopes,  
396 with highest relative amounts in skeleton (0.115%) and mucus (0.071%). With high densities of  
397 microorganisms, these small relative percentages of *Mycoplasma* and TM7 may still translate in  
398 significant numbers. Moreover, the percentages we found for TM7 may be severe underestimations  
399 because the primers we used have a low coverage for Candidate divisions WS6, TM7 and OP11  
400 (Klindworth et al., 2013). In our samples of freshly collected mucus, the genera Alteromonadaceae



401 BD1-7 clade (22%) and *Acinetobacter* (9%) were highly represented, and also *Endozoicomonas*,  
402 *Polaribacter*, *Pseudomonas*, *Aquabacterium* and *Thalassospira* were outstanding in mucus.  
403 Representatives of *Acinetobacter* have been reported from cold-water coral (Hansson et al., 2009)  
404 and from both healthy and diseased tropical corals (Koren and Rosenberg, 2008; Luna et al., 2010;  
405 Rohwer et al., 2002). Members of this genus are well known for their resistance to numerous  
406 antibiotics (Devi et al., 2011) and may play a role in the defensive-tactics of corals (Shnit-Orland and  
407 Kushmaro, 2009). *Pseudomonas* strains are also known for their antibacterial activity (Ye and Karn,  
408 2015) and this genus has been found before in *L. pertusa* (Emblem et al., 2012) and in soft corals  
409 (Salasia and Lämmner, 2008).

410 *Endozoicomonas* contains aerobic and halophilic members reported to have associations with corals  
411 (Alsheikh-Hussain, 2011; Bayer et al., 2013; Hansson et al., 2009; Kellogg et al., 2009; Pike et al.,  
412 2013; Yang et al., 2010) and other marine invertebrates (Kurahashi and Yokota, 2007; Nishijima et al.,  
413 2013). Recent results of Ainsworth et al. (2015) indicate that Endozoicimonaceae are likely localized  
414 to either the outer coral surface mucus layer or the coral skeleton, as they were found exclusively in  
415 the whole organism microbiome and not in isolated coral tissues. Our results confirm that both the  
416 mucus (1.5%) and uneroded (recently deceased coral) skeleton (0.9%) are habitats for  
417 *Endozoicomonas*. The *Endozoicomonas* found in near-bottom water (0.2%) is probably also related to  
418 the presence of mucus. *L. pertusa* is able to produce large amounts of mucus that partly dissolve in  
419 the water and stimulated oxygen consumption and microbial activity in near-bottom water up to 10x  
420 that in overlaying water (Wild et al., 2008). In this sense *Endozoicomonas* may be an indicator for  
421 reef or framework water; the genus was not found in sediment, nor in overlaying water at 5 and 10  
422 mab.

423 Different microbial communities were associated with uneroded skeleton compared to eroded  
424 skeleton. The microbial community apparently undergoes a major shift upon the death of the coral  
425 host, and continues to change as the skeleton degrades over time. This is congruent with reports on  
426 microbial succession in shallow-water tropical scleractinians that compare live tissue to recently

427 denuded coral skeleton (Le Campion-Alsumard et al., 1995). Schöttner et al. (2009) identified distinct  
428 microbial communities on different areas along a single branch of *L. pertusa*, pointing to cold-water  
429 coral framework forming a highly heterogeneous environment.

430 The variations between the different biotopes and within the biotopes that were sampled during this  
431 study, emphasize that increasing insight in the role of microbes in cold-water coral ecosystems  
432 requires both improved taxonomic resolution and actual knowledge of local biotopes, hydrography  
433 and chemical oceanography. Although our study of this single carbonate mound is among few that  
434 integrate information on hydrography with microbiology, it has for practical and logistic reasons by  
435 no means been exhaustive, and numerous pathways of future research are still open. These include  
436 further exploration of the diversity of microbial communities associated with living coral tissue, and  
437 the potential reliance of cold-water corals on their microbial associates for chemically-produced  
438 energy (Ainsworth et al., 2010; Dinsdale and Rohwer, 2011; Kellogg et al., 2009; Rohwer and Kelley,  
439 2004). Also interactions with chemical oceanography (e.g. nutrients, oxygen gradients) need to be  
440 explored similarly as with specific epifaunal organisms, especially sponges. Furthermore,  
441 comparisons on somewhat larger scale between the prominent Haas Mound and nearby mounds of  
442 smaller dimensions may shed light on the specific roles of microbes in mound development.

443

444 **Acknowledgements.** We would like to thank the captain and crew of the RV *Pelagia* and technicians  
445 of the NIOZ for their assistance during cruises 64PE360 (2012) and 64PE377 (2013),  
446 and Hans Malschaert for Linux support. This study was funded by the NIOZ Royal Netherlands  
447 Institute for Sea Research, Texel, the Netherlands and was partially funded by the Innovational  
448 Research Incentives Scheme of the Netherlands Organization for Scientific Research (NWO  
449 VENI) awarded to FM.

450

## 451 **References**

452 Ainsworth, T., Krause, L., Bridge, T., Torda, G., Raina, J.-B., Zakrzewski, M., Gates, R. D., Padilla-  
453 Gamino, J. L., Spalding, H. L., Smith, C., Woolsey, E. S., Bourne, D. G., Bongaerts, P., Hoegh-

454 Guldberg, O., and Leggat, W.: The coral core microbiome identifies rare bacterial taxa as  
455 ubiquitous endosymbionts, *ISME J.*, 2015.

456 Ainsworth, T. D., Thurber, R. V., and Gates, R. D.: The future of coral reefs: a microbial perspective,  
457 *Trends Ecol. Evol.*, 25, 233-240, 2010.

458 Alsheikh-Hussain, A.: Spatial Exploration and Characterization of Endozoicomonas spp. Bacteria in  
459 *Stylophora pistillata* Using Fluorescence In Situ Hybridization, King Abdullah University, Thesis,  
460 2011.

461 Bayer, T., Arif, C., Ferrier-Pagès, C., Zoccola, D., Aranda, M., and Voolstra, C. R.: Bacteria of the genus  
462 *Endozoicomonas* dominate the microbiome of the Mediterranean gorgonian coral *Eunicella*  
463 *cavolini*, *Mar. Ecol-Prog. Ser.*, 479, 75-84, 2013.

464 Biber, M. F., Duineveld, G. C. A., Lavaleye, M. S. S., Davies, A. J., Bergman, M. J. N., and van den Beld,  
465 I. M. J.: Investigating the association of fish abundance and biomass with cold-water corals in the  
466 deep Northeast Atlantic Ocean using a generalised linear modelling approach, *Deep Sea Res. Pt II*,  
467 99, 134-145, 2014.

468 Bongiorno, L., Mea, M., Gambi, C., Pusceddu, A., Taviani, M., and Danovaro, R.: Deep-water  
469 scleractinian corals promote higher biodiversity in deep-sea meiofaunal assemblages along  
470 continental margins, *Biol. Conserv.*, 143, 1687-1700, 2010.

471 Caporaso, J. G., Kuczynski, J., Stombaugh, J., Bittinger, K., Bushman, F. D., Costello, E. K., Fierer, N.,  
472 Pena, A. G., Goodrich, J. K., Gordon, J. I., Huttley, G. A., Kelley, S. T., Knights, D., Koenig, J. E., Ley,  
473 R. E., Lozupone, C. A., McDonald, D., Muegge, B. D., Pirrung, M., Reeder, J., Sevinsky, J. R.,  
474 Tumbaugh, P. J., Walters, W. A., Widmann, J., Yatsunenko, T., Zaneveld, J., and Knight, R.: QIIME  
475 allows analysis of high-throughput community sequencing data, *Nature Methods*, 7, 335-336,  
476 2010.

477 Carlos, C., Torres, T. T., and Ottoboni, L. M. M.: Bacterial communities and species-specific  
478 associations with the mucus of Brazilian coral species, *Scientific Reports*, 3,  
479 doi:10.1038/srep01624, 2013.

480 Claesson, M. J., O'Sullivan, O., Wang, Q., Nikkilä, J., Marchesi, J. R., Smidt, H., de Vos, W. M., Ross, R.  
481 P., and O'Toole, P. W.: Comparative analysis of pyrosequencing and a phylogenetic microarray for  
482 exploring microbial community structures in the human distal intestine, *PloS one*, 4, doi:  
483 10.1371/journal.pone.0006669 9, 2009.

484 Clarke, K. and PRIMER, G. R.: V6: user manual/tutorial, Primer-E Ltd. Plymouth.—2006, 2006.

485 Clarke, K. R.: Non-parametric multivariate analyses of changes in community structure., *Austral. J.*  
486 *Ecol.*, 18, 117-143, 1993.

487 Clarke, K. R. and Gorley, R. N.: Primer v6: user manual/tutorial., Plymouth, 2006.

488 Cole, J. R., Wang, Q., Fish, J. A., Chai, B., McGarrell, D. M., Sun, Y., Brown, C. T., Porras-Alfaro, A.,  
489 Kuske, C. R., and Tiedje, J. M.: Ribosomal Database Project: data and tools for high throughput  
490 rRNA analysis, *Nucleic Acids Res.*, 42, D633-D642, 2014.

491 Costello, M. J., McCrea, M., Freiwald, A., Lundälv, T., Jonsson, L., Bett, B. J., van Weering, T. C., de  
492 Haas, H., Roberts, J. M., and Allen, D.: Role of cold-water *Lophelia pertusa* coral reefs as fish  
493 habitat in the NE Atlantic. In: *Cold-water corals and ecosystems*, Springer, Heidelberg, Germany  
494 2005.

495 De Caceres, M. and Legendre, P.: Associations between species and groups of sites: indices and  
496 statistical inference, *Ecology*, 90, 3566-3574, 2009.

497 De Haas, H., Mienis, F., Frank, N., Richter, T. O., Steinacher, R., De Stigter, H., Van der Land, C., and  
498 Van Weering, T. C.: Morphology and sedimentology of (clustered) cold-water coral mounds at the  
499 south Rockall Trough margins, NE Atlantic Ocean, *Facies*, 55, 1-26, 2009.

500 Devi, P., Wahidulla, S., Kamat, T., and D'Souza, L.: Screening marine organisms for antimicrobial  
501 activity against clinical pathogens, *Indian J. Mar. Sci.*, 40, 338-346, 2011.

502 Dinsdale, E. A. and Rohwer, F.: Fish or germs? Microbial dynamics associated with changing trophic  
503 structures on coral reefs. In: *Coral Reefs: An Ecosystem in Transition*, Springer, Heidelberg,  
504 Germany, 2011.

505 Dufrene, M. and Legendre, P.: Species assemblages and indicator species: The need for a flexible  
506 asymmetrical approach, *Ecol. Monogr.*, 67, 345-366, 1997.

507 Duineveld, G. C., Lavaleye, M. S., Bergman, M. J., De Stigter, H., and Mienis, F.: Trophic structure of a  
508 cold-water coral mound community (Rockall Bank, NE Atlantic) in relation to the near-bottom  
509 particle supply and current regime, *B. Mar. Sci.*, 81, 449-467, 2007.

510 Emblem, A., Karlsen, B. O., Evertsen, J., Miller, D. J., Moum, T., and Johansen, S. D.: Mitogenome  
511 polymorphism in a single branch sample revealed by SOLiD deep sequencing of the *Lophelia*  
512 *pertusa* coral genome, *Gene*, 506, 344-349, 2012.

513 Findlay, H. S., Hennige, S. J., Wicks, L. C., Navas, J. M., Woodward, E. M. S., and Roberts, J. M.: Fine-  
514 scale nutrient and carbonate system dynamics around cold-water coral reefs in the northeast  
515 Atlantic, *Scientific reports*, 4, doi:10.1038/srep03671, 2014.

516 Galkiewicz, J. P., Pratte, Z. A., Gray, M. A., and Kellogg, C. A.: Characterization of culturable bacteria  
517 isolated from the cold-water coral *Lophelia pertusa*, *FEMS Microbiol. Ecol.*, 77, 333-346, 2011.

518 Genin, A., Yahel, G., Reidenbach, M. A., Monismith, S. B., and Koseff, J. R.: Intense benthic grazing on  
519 phytoplankton in coral reefs revealed using the control volume approach., *Oceanography*, 15, 90-  
520 96, 2002.

521 Gilbert, J. A., Hill, R., Doblin, M. A., and Ralph, P. J.: Microbial consortia increase thermal tolerance of  
522 corals, *Mar. Biol.*, 159, 1763-1771, 2012.

523 Hansson, L., Agis, M., Maier, C., and Weinbauer, M. G.: Community composition of bacteria  
524 associated with cold-water coral *Madrepora oculata*: within and between colony variability, *Mar.*  
525 *Ecol. Prog. Ser.*, 397, 89-102, 2009.

526 Henry, L.-A. and Roberts, J. M.: Biodiversity and ecological composition of macrobenthos on cold-  
527 water coral mounds and adjacent off-mound habitat in the bathyal Porcupine Seabight, NE  
528 Atlantic, *Deep Sea Res. Pt I*, 54, 654-672, 2007.

529 Jensen, S., Bourne, D. G., Hovland, M., and Murrell, J. C.: High diversity of microplankton surrounds  
530 deep-water coral reef in the Norwegian Sea, *Fems Microbiol. Ecol.*, 82, 75-89, 2012.

531 Jensen, S., Lynch, M. D. J., Ray, J. L., Neufeld, J. D., and Hovland, M.: Norwegian deep-water coral  
532 reefs: cultivation and molecular analysis of planktonic microbial communities, *Environ. Microbiol.*,  
533 DOI: 10.1111/1462-2920.12531, 2014.

534 Jensen, S., Neufeld, J. D., Birkeland, N.-K., Hovland, M., and Murrell, J. C.: Insight into the microbial  
535 community structure of a Norwegian deep-water coral reef environment, *Deep Sea Res. Pt I*, 55,  
536 1554-1563, 2008.

537 Kellogg, C. A., Lisle, J. T., and Galkiewicz, J. P.: Culture-independent characterization of bacterial  
538 communities associated with the cold-water coral *Lophelia pertusa* in the northeastern Gulf of  
539 Mexico, *Appl. Environ. Microb.*, 75, 2294-2303, 2009.

540 Kenyon, N. H., Akhmetzhanov, A. M., Wheeler, A. J., van Weering, T. C., de Haas, H., and Ivanov, M.  
541 K.: Giant carbonate mud mounds in the southern Rockall Trough, *Mar. Geol.*, 195, 5-30, 2003.

542 Klindworth, A., Pruesse, E., Schweer, T., Peplies, J., Quast, C., Horn, M., and Glöckner, F. O.:  
543 Evaluation of general 16S ribosomal RNA gene PCR primers for classical and next-generation  
544 sequencing-based diversity studies, *Nucleic Acids Res.*, 41, e1-e1, 2013.

545 Knowlton, N. and Rohwer, F.: Multispecies microbial mutualisms on coral reefs: the host as a habitat,  
546 *Am. Nat.*, 162, S51-S62, 2003.

547 Koren, O. and Rosenberg, E.: Bacteria associated with the bleached and cave coral *Oculina*  
548 *patagonica*, *Microbial Ecol.*, 55, 523-529, 2008.

549 Krediet, C. J., Ritchie, K. B., Alagely, A., and Teplitski, M.: Members of native coral microbiota inhibit  
550 glycosidases and thwart colonization of coral mucus by an opportunistic pathogen, *ISME J*, 7, 980-  
551 990, 2013.

552 Kurahashi, M. and Yokota, A.: *Endozoicomonas elysicola* gen. nov., sp nov., a gamma-  
553 proteobacterium isolated from the sea slug *Elysia ornata*, *Syst. Appl. Microbiol.*, 30, 202-206,  
554 2007.

555 Le Campion-Alsumard, T., Golubic, S., and Hutchings, P.: Microbial endoliths in skeletons of live and  
556 dead corals - *Porites lobata* (Moorea, French-Polynesia). *Mar. Ecol. Progr. Ser.*, 117, 149-157,  
557 1995.

558 Luna, G. M., Bongiorno, L., Gili, C., Biavasco, F., and Danovaro, R.: *Vibrio harveyi* as a causative agent  
559 of the White Syndrome in tropical stony corals, *Environ. Microbiol.*, 2, 120-127, 2010.

560 Mienis, F., De Stigter, H. C., White, M., Duineveld, G., De Haas, H., and Van Weering, T. C. E.:  
561 Hydrodynamic controls on cold-water coral growth and carbonate-mound development at the SW  
562 and SE Rockall Trough Margin, NE Atlantic Ocean, *Deep Sea Res. Pt I*, 54, 1655-1674, 2007.

563 Mienis, F., Van Weering, T., De Haas, H., De Stigter, H., Huvenne, V., and Wheeler, A.: Carbonate  
564 mound development at the SW Rockall Trough margin based on high resolution TOBI and seismic  
565 recording, *Mar. Geol.*, 233, 1-19, 2006.

566 Mohn, C., Rengstorf, A., White, M., Duineveld, G., Mienis, F., Soetaert, K., and Grehan, A.: Linking  
567 benthic hydrodynamics and cold-water coral occurrences: A high-resolution model study at three  
568 cold-water coral provinces in the NE Atlantic, *Progr. Oceanogr.*, 122, 92-104, 2014.

569 Neulinger, S. C., Gaertner, A., Jarnegren, J., Ludvigsen, M., Lochte, K., and Dullo, W.-C.: Tissue-  
570 Associated "Candidatus *Mycoplasma corallicola*" and Filamentous Bacteria on the Cold-Water  
571 Coral *Lophelia pertusa* (Scleractinia), *Applied and Environmental Microbiology*, 75, 1437-1444,  
572 2009.

573 Neulinger, S. C., Järnegren, J., Ludvigsen, M., Lochte, K., and Dullo, W.-C.: Phenotype-specific  
574 bacterial communities in the cold-water coral *Lophelia pertusa* (Scleractinia) and their  
575 implications for the coral's nutrition, health, and distribution, *Appl. Environ. Microbiol.*, 74, 7272-  
576 7285, 2008.

577 Nishijima, M., Adachi, K., Katsuta, A., Shizuri, Y., and Yamasato, K.: *Endozoicomonas numazuensis* sp.  
578 nov., a gammaproteobacterium isolated from marine sponges, and emended description of the  
579 genus *Endozoicomonas* Kurahashi and Yokota 2007, *Int. J. Syst. Evol. Micr.*, 63, 709-714, 2013.

580 Penn, K., Wu, D., Eisen, J. A., and Ward, N.: Characterization of bacterial communities associated with  
581 deep-sea corals on Gulf of Alaska seamounts, *Appl. Environ. Microbiol.*, 72, 1680-1683, 2006.

582 Pike, R. E., Haltli, B., and Kerr, R. G.: *Endozoicomonas euniceicola* sp. nov. and *Endozoicomonas*  
583 *gorgoniicola* sp. nov., bacteria isolated from the octocorals, *Eunicea fusca* and *Plexaura* sp., *Int. J.*  
584 *Syst. Evol. Micr.*, 63, doi: 10.1099/ijs.0.051490-02013.

585 Reidenbach, M. A., Monismith, S. G., Koseff, J. R., Yahel, G., and Genin, A.: Boundary layer turbulence  
586 and flow structure over a fringing coral reef, *Limnol. Oceanogr.*, 51, 1956-1968, 2006.

587 Rohwer, F. and Kelley, S.: Culture-independent analyses of coral-associated microbes. In: *Coral health*  
588 *and disease*, Springer, Heidelberg, Germany, 265-277, 2004.

589 Rohwer, F., Seguritan, V., Azam, F., and Knowlton, N.: Diversity and distribution of coral-associated  
590 bacteria, *Mar. Ecol. Progr. Ser.*, 243, 1-10, 2002.

591 Rosenberg, E., Kellogg, C. A., and Rohwer, F.: *Coral microbiology*, Washington, 146pp., 2007.

592 Rovelli, L., Attard, K. M., Bryant, L. D., Floegel, S., Stahl, H., Roberts, J. M., Linke, P., and Glud, R. N.:  
593 Benthic O<sub>2</sub> uptake of two cold-water coral communities estimated with the non-invasive eddy  
594 correlation technique, *Mar. Ecol. Progr. Ser.*, 525, 97-104, 2015.

595 Salasia, S. and Lämmle, C.: Antibacterial property of marine *Bacterium pseudomonas* sp. associated  
596 with a soft coral against pathogenic *Streptococcus equi* subsp. *zooeconomicus*, *J. Coastal*  
597 *Developm.* 11, 113-120, 2008.

598 Schöttner, S., Hoffmann, F., Wild, C., Rapp, H. T., Boetius, A., and Ramette, A.: Inter-and intra-habitat  
599 bacterial diversity associated with cold-water corals, *ISME J.*, 3, 756-759, 2009.

600 Schöttner, S., Wild, C., Hoffmann, F., Boetius, A., and Ramette, A.: Spatial scales of bacterial diversity  
601 in cold-water coral reef ecosystems, *PloS one*, 7, doi: 10.1371/journal.pone.00320, 2012.

602 Shnit-Orland, M. and Kushmaro, A.: Coral mucus-associated bacteria: a possible first line of defense,  
603 *FEMS Microbiol. Ecol.*, 67, 371-380, 2009.

604 Templer, S. P., Wehrmann, L. M., Zhang, Y., Vasconcelos, C., and McKenzie, J. A.: Microbial  
605 community composition and biogeochemical processes in cold-water coral carbonate mounds in  
606 the Gulf of Cadiz, on the Moroccan margin, *Mar. Geo.*, 282, 138-148, 2011.

607 van Haren, H., Mienis, F., Duineveld, G. C., and Lavaleye, M. S.: High-resolution temperature  
608 observations of a trapped nonlinear diurnal tide influencing cold-water corals on the Logachev  
609 mounds, *Progr. Oceanogr.*, 125, 16-25, 2014.

610 van Oevelen, D., Duineveld, G., Lavaleye, M., Mienis, F., Soetaert, K., and Heip, C. H.: The cold-water  
611 coral community as a hot spot for carbon cycling on continental margins: A food-web analysis  
612 from Rockall Bank (northeast Atlantic), *Limnol. Oceanogr.*, 54, 1829-1844, 2009.

613 van Soest, R. W., Cleary, D. F., de Kluijver, M. J., Lavaleye, M. S., Maier, C., and van Duyl, F. C.: Sponge  
614 diversity and community composition in Irish bathyal coral reefs, *Contrib. Zool.*, 76, 121-142,  
615 2008.

616 van Weering, T. C., De Haas, H., De Stigter, H., Lykke-Andersen, H., and Kouvaev, I.: Structure and  
617 development of giant carbonate mounds at the SW and SE Rockall Trough margins, NE Atlantic  
618 Ocean, *Mar. Geol.*, 198, 67-81, 2003.

619 Wang, Q., Garrity, G. M., Tiedje, J. M., and Cole, J. R.: Naive Bayesian classifier for rapid assignment of  
620 rRNA sequences into the new bacterial taxonomy, *Appl. Environ. Microbiol.*, 73, 5261-5267, 2007.

621 Wild, C., Mayr, C., Wehrmann, L., Schöttner, S., Naumann, M., Hoffmann, F., and Rapp, H. T.: Organic  
622 matter release by cold water corals and its implication for fauna-microbe interaction, *Mar. Ecol.*  
623 *Prog. Ser.*, 372, 67-75, 2008.

624 Yakimov, M. M., Cappello, S., Crisafi, E., Tursi, A., Savini, A., Corselli, C., Scarfi, S., and Giuliano, L.:  
625 Phylogenetic survey of metabolically active microbial communities associated with the deep-sea  
626 coral *Lophelia pertusa* from the Apulian plateau, Central Mediterranean Sea, *Deep Sea Res. Pt I*,  
627 53, 62-75, 2006.

628 Yang, C.-S., Chen, M.-H., Arun, A., Chen, C. A., Wang, J.-T., and Chen, W.-M.: *Endozoicomonas*  
629 *montiporae* sp. nov., isolated from the encrusting pore coral *Montipora aequituberculata*, *Int. J.*  
630 *Syst. Evol. Micr.*, 60, 1158-1162, 2010.

631 Ye, F. and Karn, J.: Bacterial Short Chain Fatty Acids Push All The Buttons Needed To Reactivate  
632 Latent Viruses, *Stem Cell Epigen.*, 2, 2015.

633

634

635 **Table 1.** Number of unique samples taken from different biotopes at Haas mound summit, slope and  
 636 off mound. Number between brackets is total number of samples analysed, including replicates.

<b>Biotope</b>	<b>Sample type</b>	<b>summit</b>	<b>slope</b>	<b>off mound</b>	<b>total</b>
overlying water	400 m	4 (23)	2 (6)	2 (6)	8 (23)
	10 mab	3 (9)	2 (6)	2 (6)	7 (21)
	5 mab	4 (12)	2 (6)	2 (6)	8 (24)
near-bottom water	w_bc	4 (11)		1 (3)	5 (14)
skeleton	uneroded	2 (6)	2 (6)		4 (12)
	eroded	1 (3)	1 (6)		2 (9)
mucus	mucus	1 (3)	1 (3)		2 (6)
sediment	sediment	2 (6)	2 (6)		4 (12)

641 **Table 2.** List of box-core sampling stations.

Year	Site	Station nr	Latitude	Longitude	Depth (m)	Framework height (cm)	Biotope
2012	Mound slope	15	N 55° 29.45'	W 15° 48.41'	528	> 30	Mucus Skeleton-uneroded
	Summit	24	N 55° 29.77'	W 15° 48.05'	549	0-10	Near-bottom water
	Mound slope	25	N 55° 29.57'	W 15° 47.81'	568	>30	Mucus Skeleton-uneroded
	Mound slope	46	N 55° 29.45'	W 15° 47.64'	745	10-30	Near-bottom water
	Summit	72	N 55° 29.51'	W 15° 48.40'	562	0-10	Near-bottom water
2013	Mound slope	8	N 55° 29.45'	W 15° 47.64'	647	>30	Sediment
	Summit	9	N 55° 29.77'	W 15° 48.03'	547	0-10	Near-bottom water Sediment Skeleton-uneroded Skeleton-eroded
	Summit	11	N 55° 29.50'	W 15° 48.39'	564	10-30	Near-bottom water Sediment
	Mound slope	12	N 55° 29.26'	W 15° 48.45'	635	>30	Sediment Skeleton-uneroded Skeleton-eroded

642

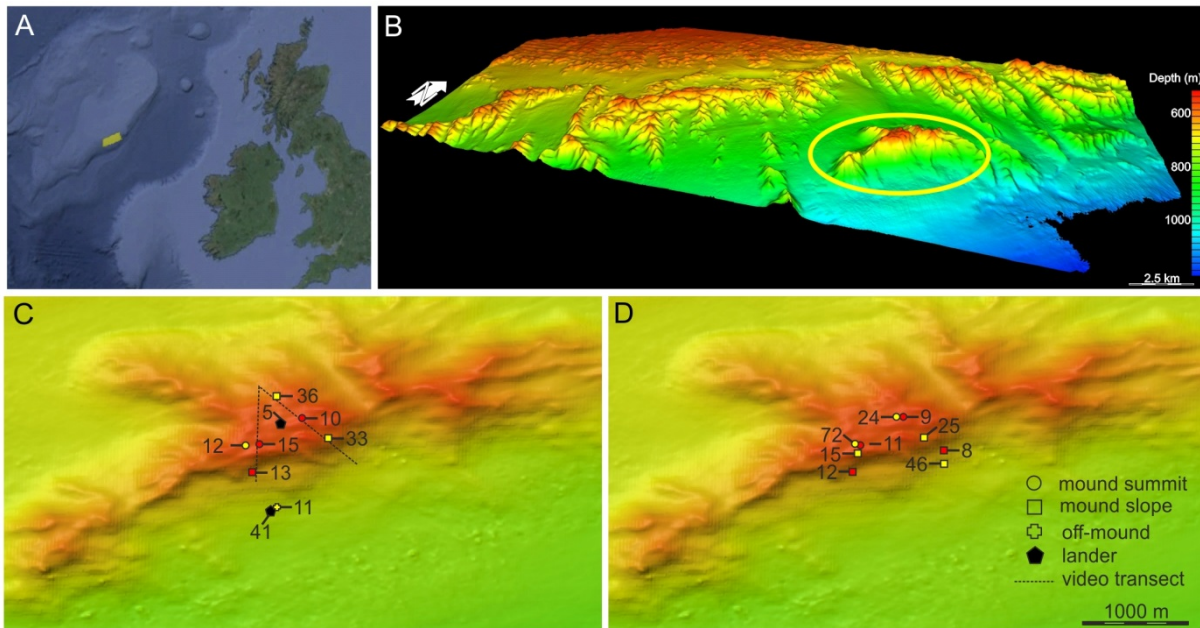
643



644 **Table 3.** List of sampling stations of the overlaying water column. See for abbreviation Fig. 5.

Year	Site	Station nr	Latitude	Longitude	Sample depth (m)	Sample type	Temperature (°C)
2012	Off mound	11	N 55° 28.92'	W 15° 48.33'	400	w_400m	9.7
					895	w_10mab	6.7
					907	w_5mab	6.6
	Mound summit	12	N 55° 29.50'	W 15° 48.50'	400	w_400m	9.6
					553	w_10mab	9
					562	w_5mab	8.9
	Mound slope	33	N 55° 29.57'	W 15° 47.83'	390	w_400m	10
					573	w_10mab	8.7
					578	w_5mab	8.6
	Mound slope	36	N 55° 29.94'	W 15° 48.29'	400	w_400m	10
					596	w_5mab	8.7
	2013	Off mound	2	N 55° 25.95'	W 15° 43.83'	400	w_400m
1192						w_10mab	5.7
1200						w_5mab	5.4
Mound summit		10	N 55° 29.76'	W 15° 48.04'	400	w_400m	9.8
					522	w_10mab	8.8
					530	w_5mab	8.5
Mound slope		13	N 55° 29.25'	W 15° 48.44'	400	w_400m	9.7
					709	w_10mab	9.1
					718	w_5mab	9.2
Mound summit		15	N 55° 29.50'	W 15° 48.39'	400	w_400m	9.8
					550	w_10mab	9
					555	w_5mab	8.9

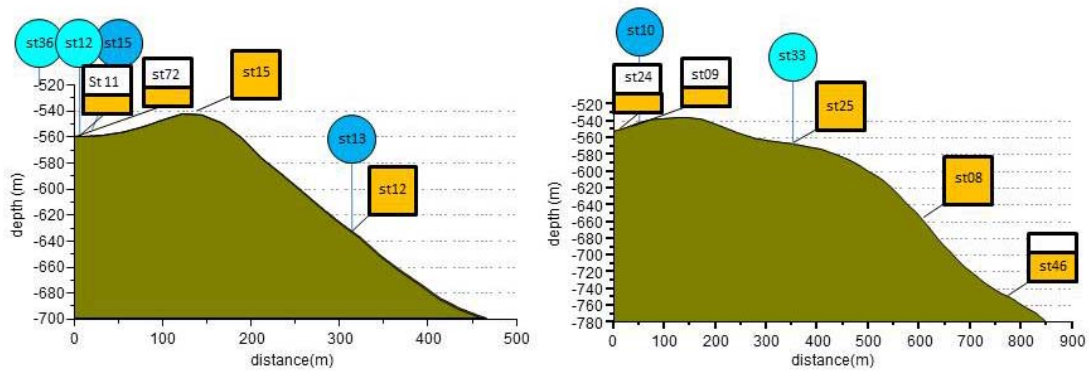
646 **Figure 1.** A. Location of Logachev Mound Province (yellow polygon). B. Multibeam map of Logachev  
647 Mounds with Haas Mound encircled. C. Detail of Haas Mound with lander and CTD stations arranged  
648 along two video transects (dotted lines). D. Detail of Haas Mound with box-corer stations indicated.  
649 Note CTD02 is not on the map and lies 8 km SE of CTD10. Red and yellow symbols indicate stations  
650 sampled in 2012 and 2013, respectively.



651 Figure 1

652

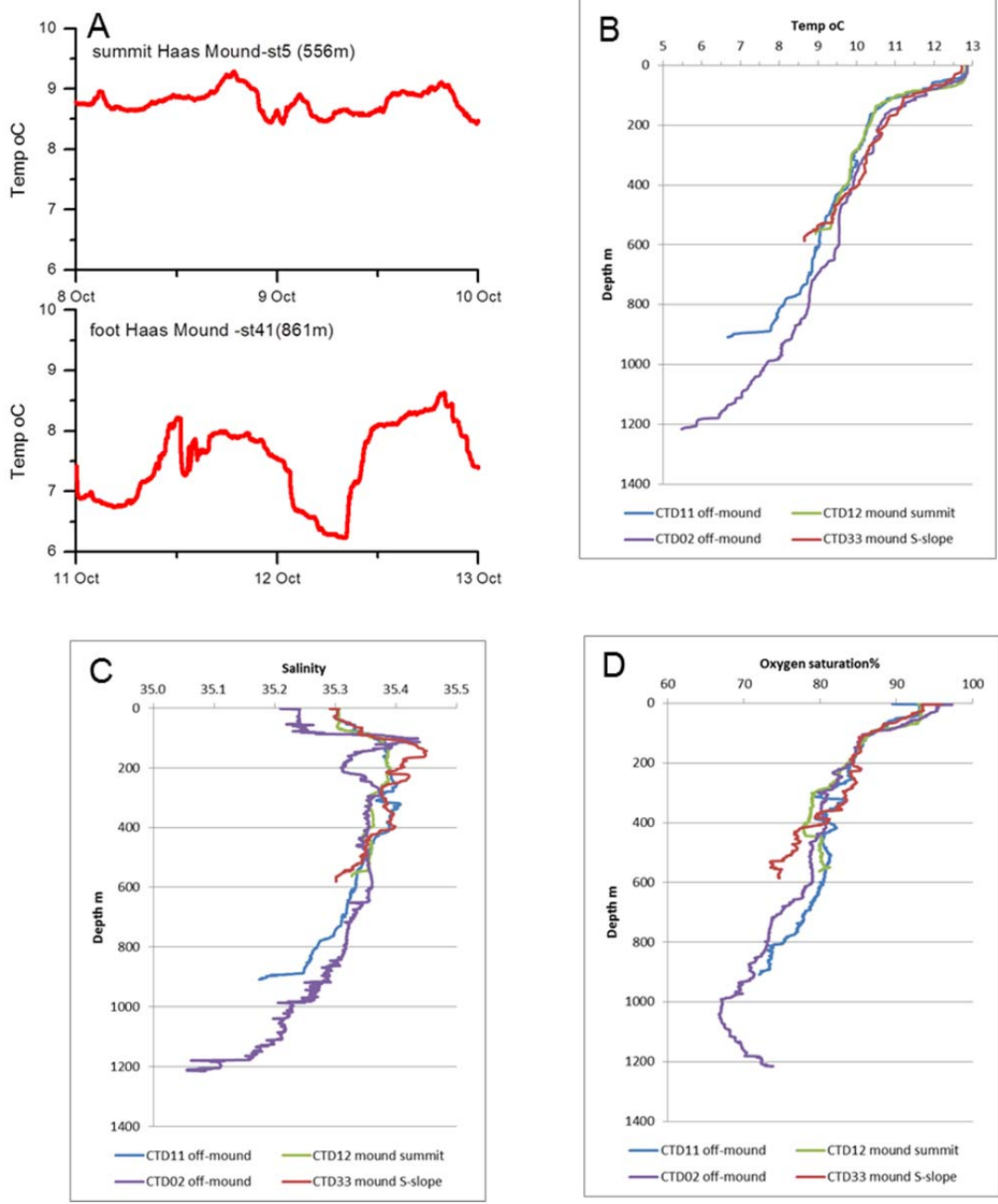
653 **Figure 2.** Bathymetric profiles of the two transects across the S-slope of Haas Mound (see Fig. 1). The  
654 position of the box-cores (squares) and some of the CTD casts (circles) is indicated. The yellow color  
655 filling of the squares represents the approximate percentage coral cover. Note that scales of x and y  
656 axes differ.



657

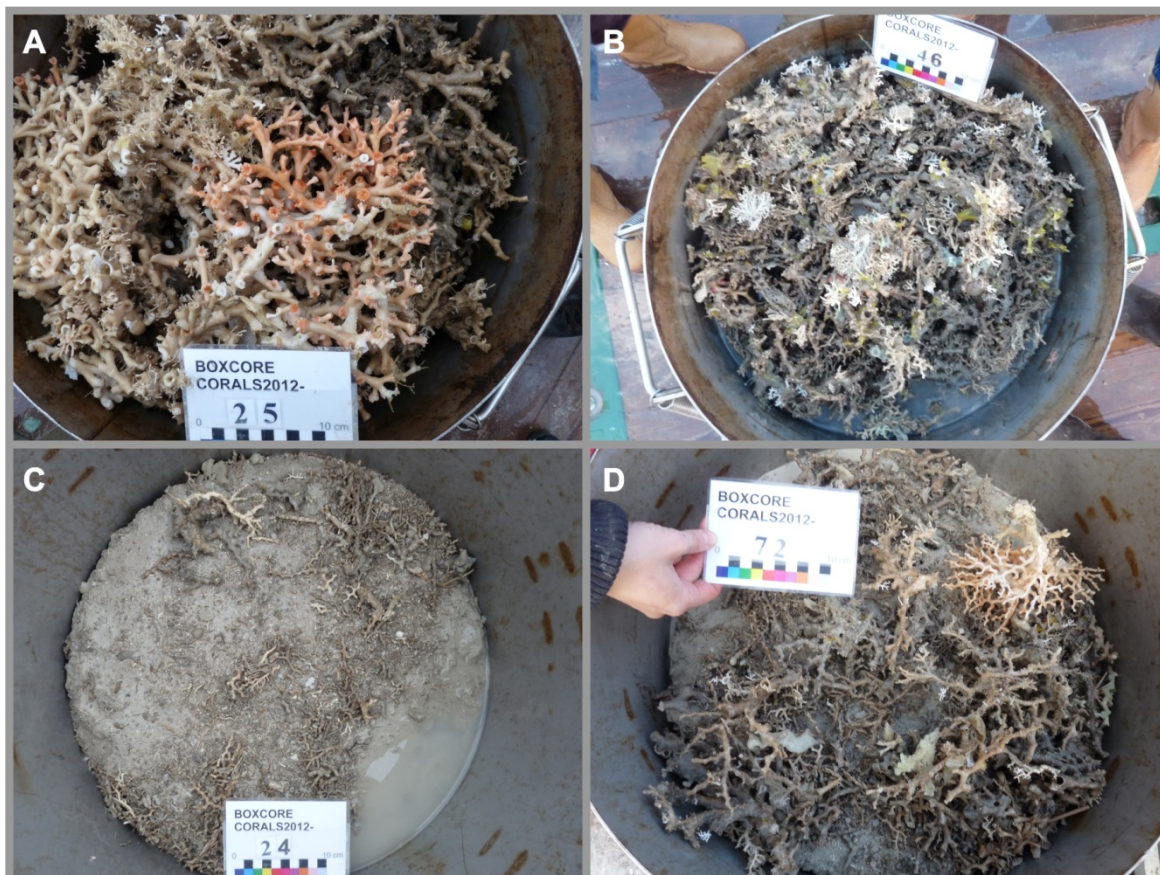
658

659 **Figure 3.** A. Temperature recorded *in situ* at the summit and foot of Haas Mound by a current meter  
 660 on a benthic lander. B-D. Salinity, Temperature (°C), and Oxygen (% saturation), respectively, as  
 661 recorded with the CTD on the slopes and summit of Haas Mound in October 2012 and 2013.



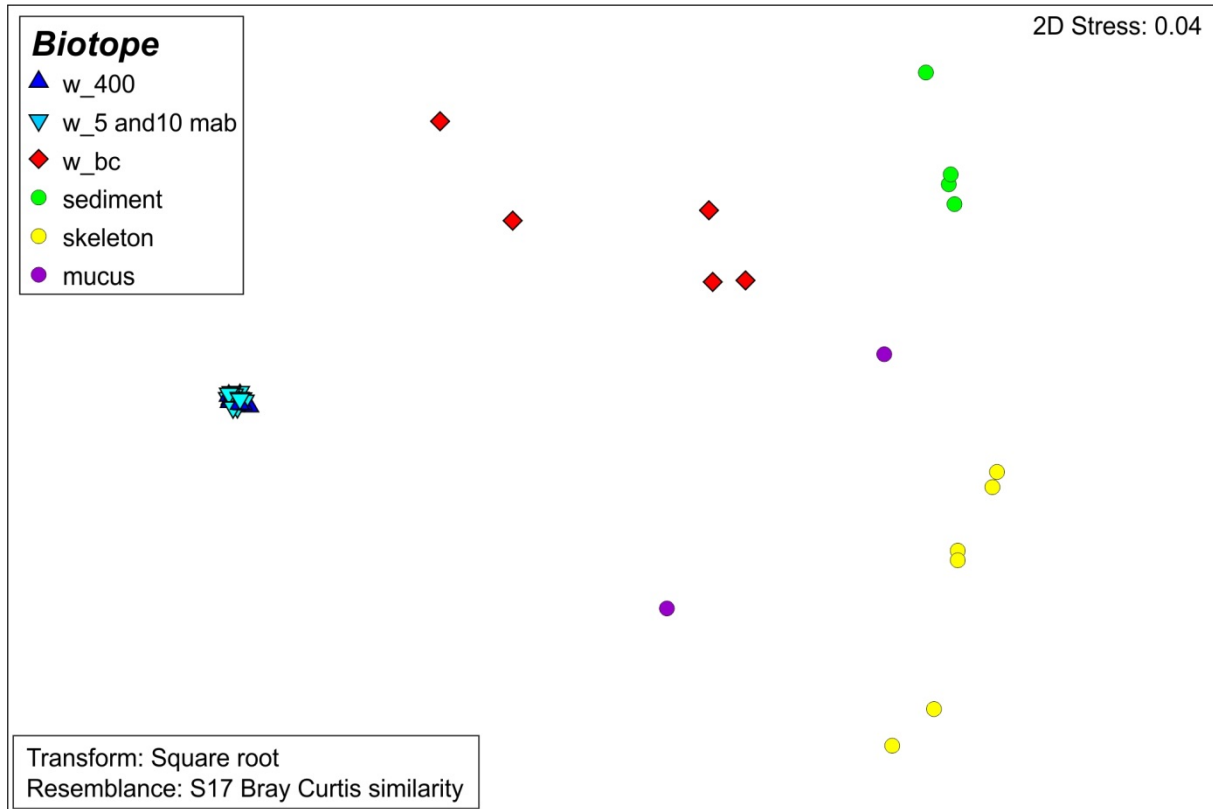
662

663 **Figure 4.** Photographs of box-cores taken at the S-slope (A, st25 and B, st46) and summit (C, st24 and  
664 D, st72) of Haas mound. A clear difference in the amount and height of coral framework was  
665 observed.



666 Figure 4

667 **Figure 5.** Microbial OTU composition of 40 samples shows clustering according to biotope: overlaying  
668 water (w\_400 m; w\_5 and 10 mab), near-bottom water (w\_bc), sediment, skeleton and mucus. The  
669 MDS plot of all 121 samples analyzed, including replicates, shows a similar pattern (S.I. Fig. 1). The  
670 same pattern is apparent for microbial classes and genera (not shown).

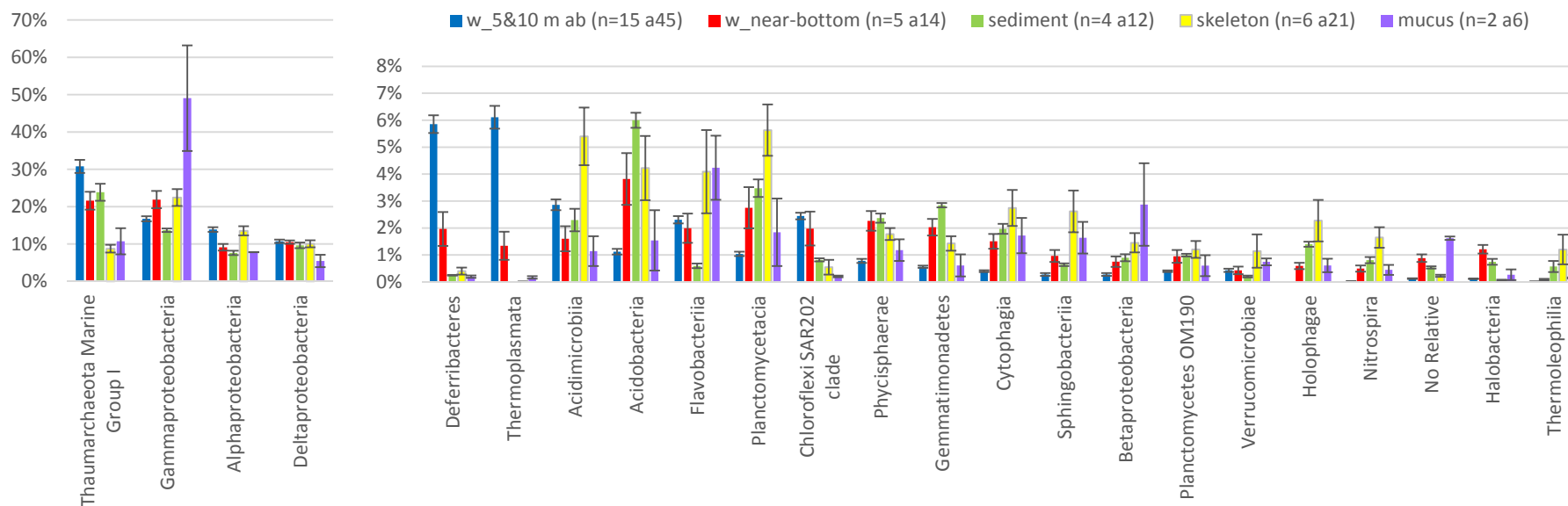


671 Figure 5

672 Figure 6. Microbial community composition of five biotopes sampled at Haas mound. N= number of unique samples per biotope with a: total number of  
 673 samples, including replicates. A. Most abundant (>1% of total reads) classes. B. Most abundant (>0.5% of total reads) genera plotted as percentage, with  
 674 standard error.

675

A



676

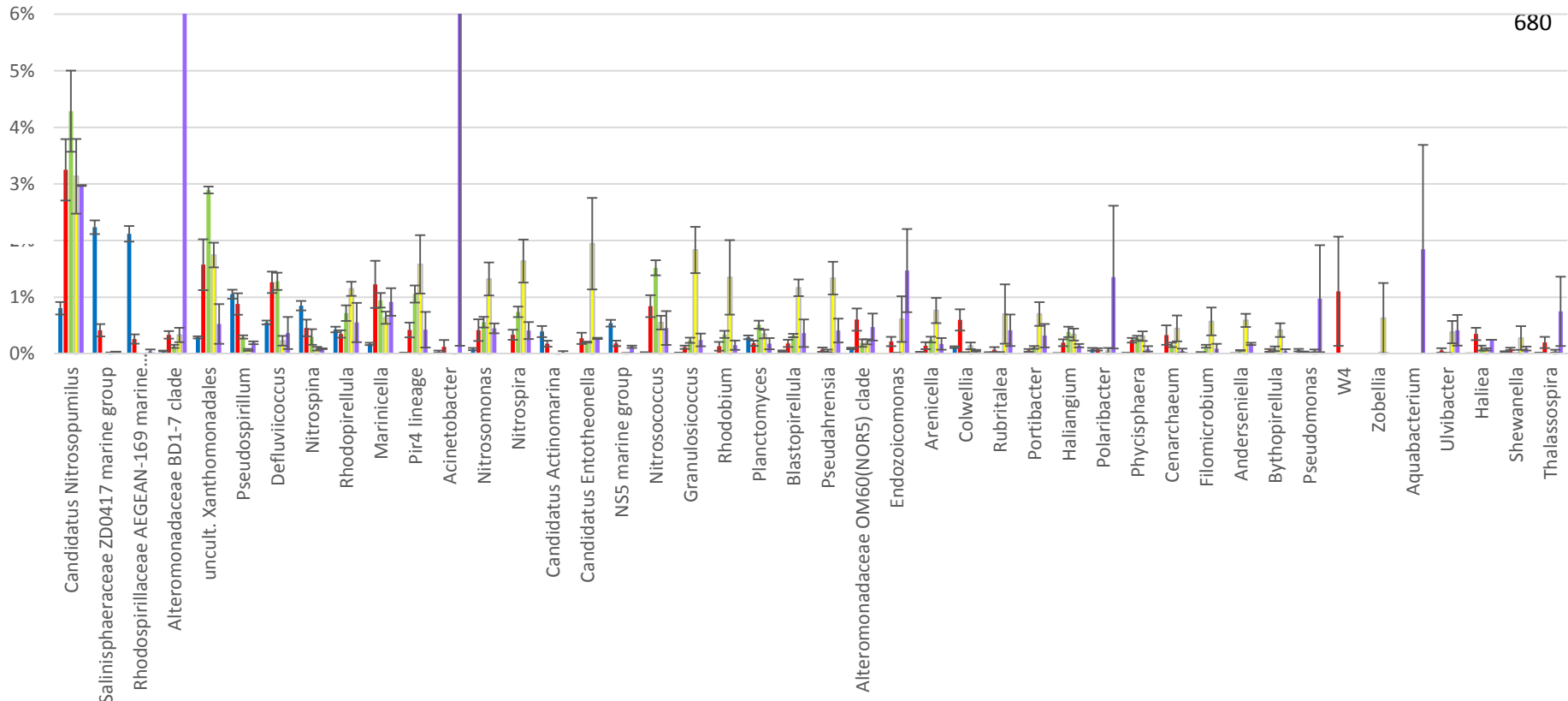
677

678

B

■ w\_5&10 m ab (n=15 a45) ■ w\_near-bottom (n=5 a14) ■ sediment (n=4 a12) ■ skeleton (n=6 a21) ■ mucus (n=2 a6)

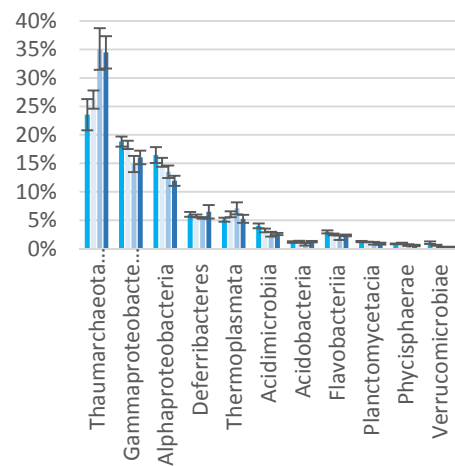
679



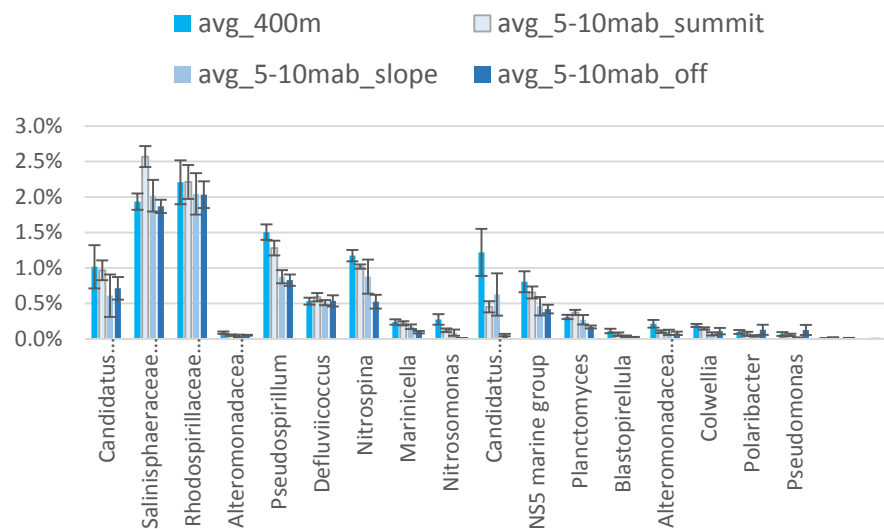


681 Figure 7. Differences in microbial community composition within biotopes. N= number of unique samples per biotope with a: total number of samples,  
 682 including replicates. A. Microbial classes for overlaying water at 400 m depth, and at 5 and 10 mab on mound summit, slope and off-mound. B. genera for  
 683 overlaying water at 400 m depth (n=8, a23), and at 5 and 10 mab on mound summit (n=7, a21), slope (n=4, a12) and off-mound (n=4, a12). C. Microbial  
 684 classes for uneroded (recently deceased) and eroded skeleton. D. genera for uneroded (recently deceased) and eroded skeleton. Values plotted as  
 685 percentage with standard error.

A

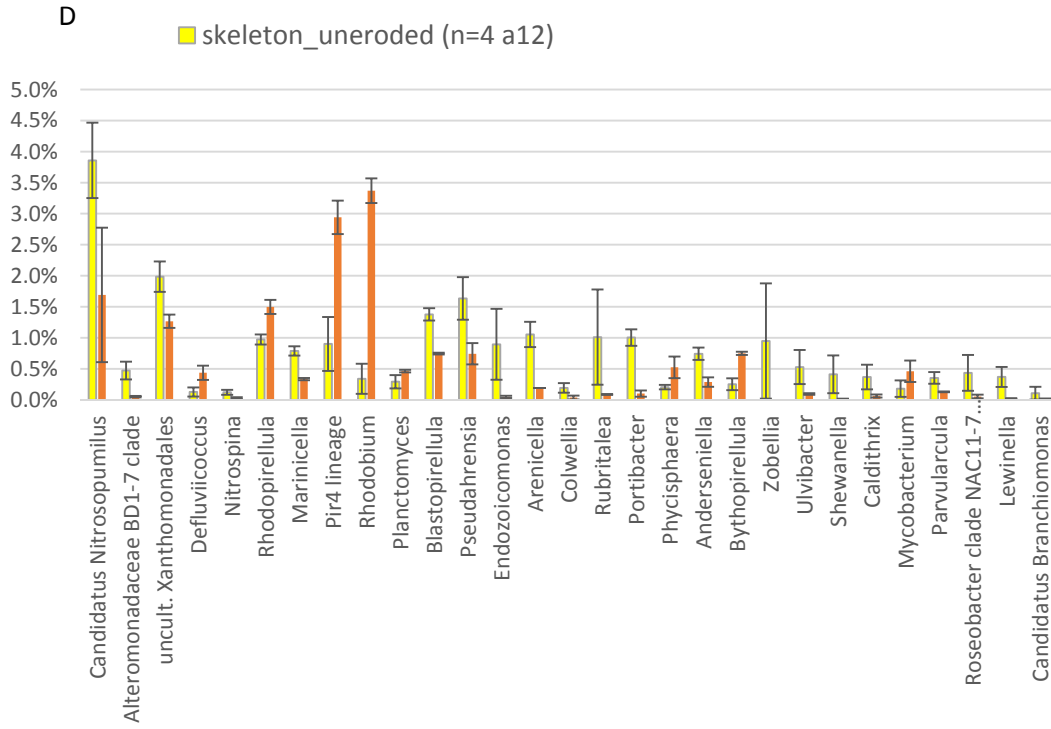
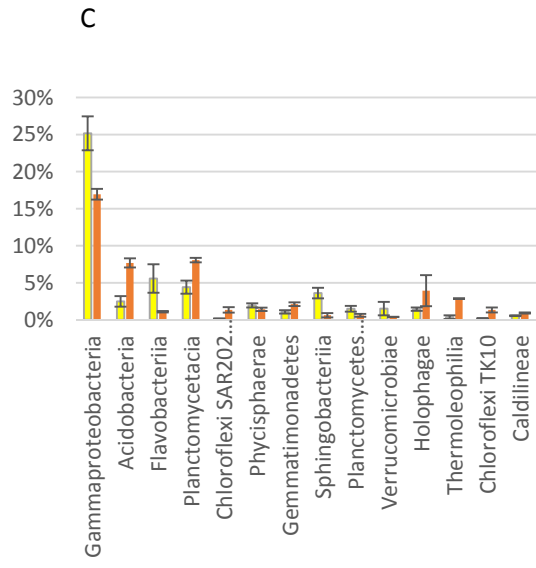


B



686

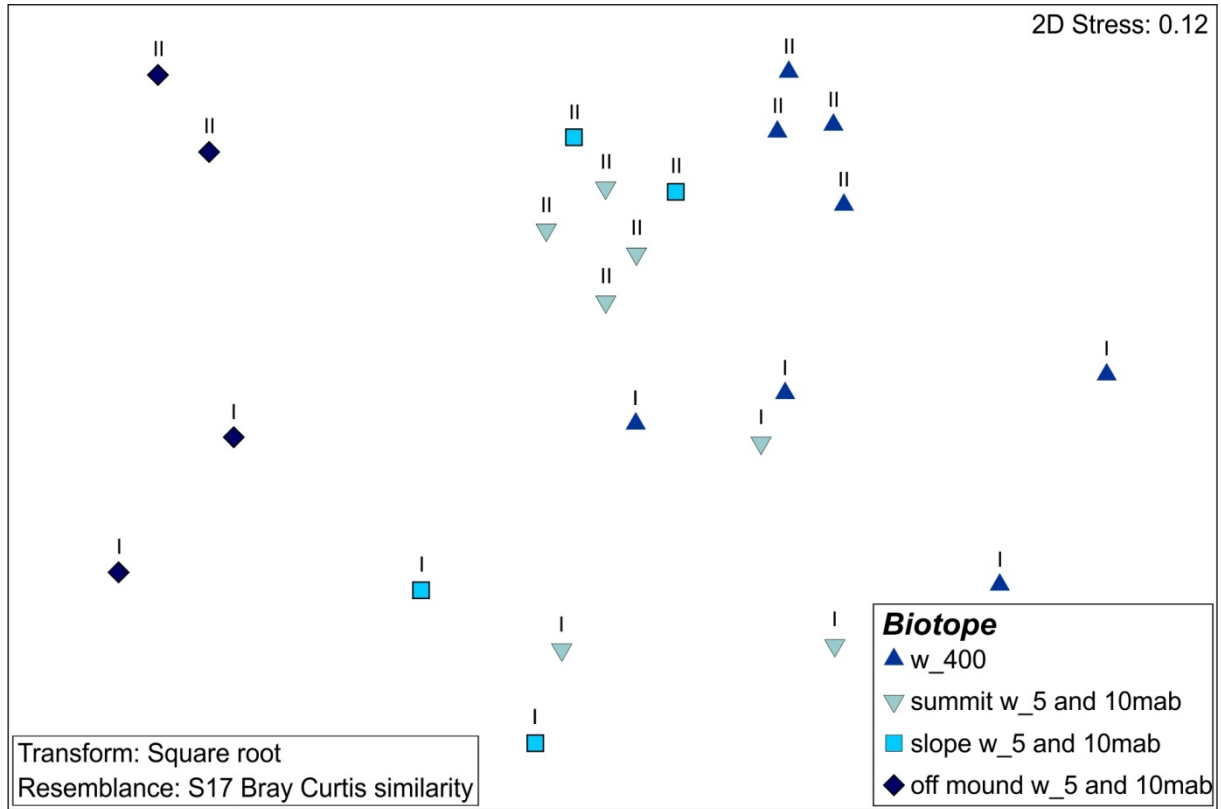
687



689 **Figure 8.** Zoom of microbial OTU composition of overlaying water (w\_400 m and w\_5 and 10 mab).

690 Roman capital I = 2012, II = 2013.

691



692 Figure 8

693

694 **Figure 9.** Zoom of microbial OTU composition of coral skeleton (eroded and uneroded). Roman  
695 capital I = 2012, II = 2013.

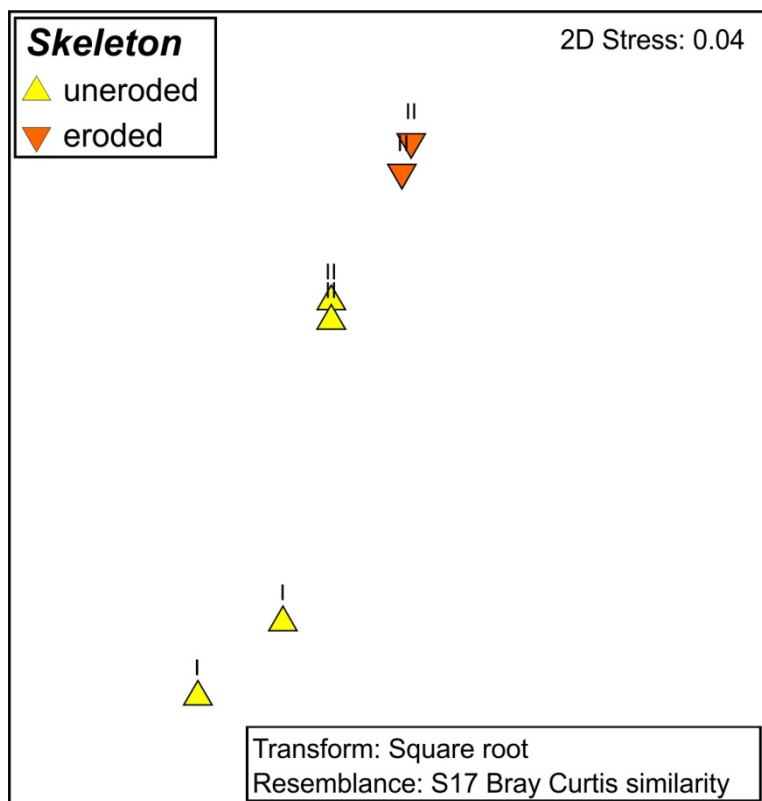


Figure 9

696

697

698

699 **Supplementary information**

700

701 **S.I. Table 1.** Sequence output and microbial diversity indices (average  $\pm$  standard error) of five

702 biotopes sampled at Haas Mound. Singletons were not excluded in this analysis.

<b>biotope</b>	<b>reads/sample</b>	<b>observed OTUs</b>	<b>Chao1</b>	<b>Shannon</b>
near-bottom water (n=5)	11456 $\pm$ 798	3858 $\pm$ 567	7876 $\pm$ 618	6.95 $\pm$ 0.09
sediment (n=4)	14070 $\pm$ 941	3245 $\pm$ 104	5357 $\pm$ 688	6.40 $\pm$ 0.16
skeleton (n=6)	17713 $\pm$ 1952	2856 $\pm$ 300	4637 $\pm$ 709	6.19 $\pm$ 0.07
mucus (n=2)	20140 $\pm$ 2229	2663 $\pm$ 665	2828 $\pm$ 1123	4.93 $\pm$ 0.87
overlying water (n=23)	17651 $\pm$ 1599	1712 $\pm$ 119	2684 $\pm$ 306	5.04 $\pm$ 0.06

703

704

705

706 **S.I. Table 2.** Indicator taxa given for five biotopes sampled at Haas Mound. Only those with the  
707 highest statistics values are listed. Numbers between brackets are number of strong indicators  
708 (A>0.85) over the total number of significant indicators (p<0.0001) found. w\_CTD = water sampled at  
709 400 m and 5 and 10 mab; Near-bottom water (w\_bc). A = given the indicator is present, the  
710 probability that the sample belongs to the sample group. B = taking one sample from the group, the  
711 probability that it contains the indicator.

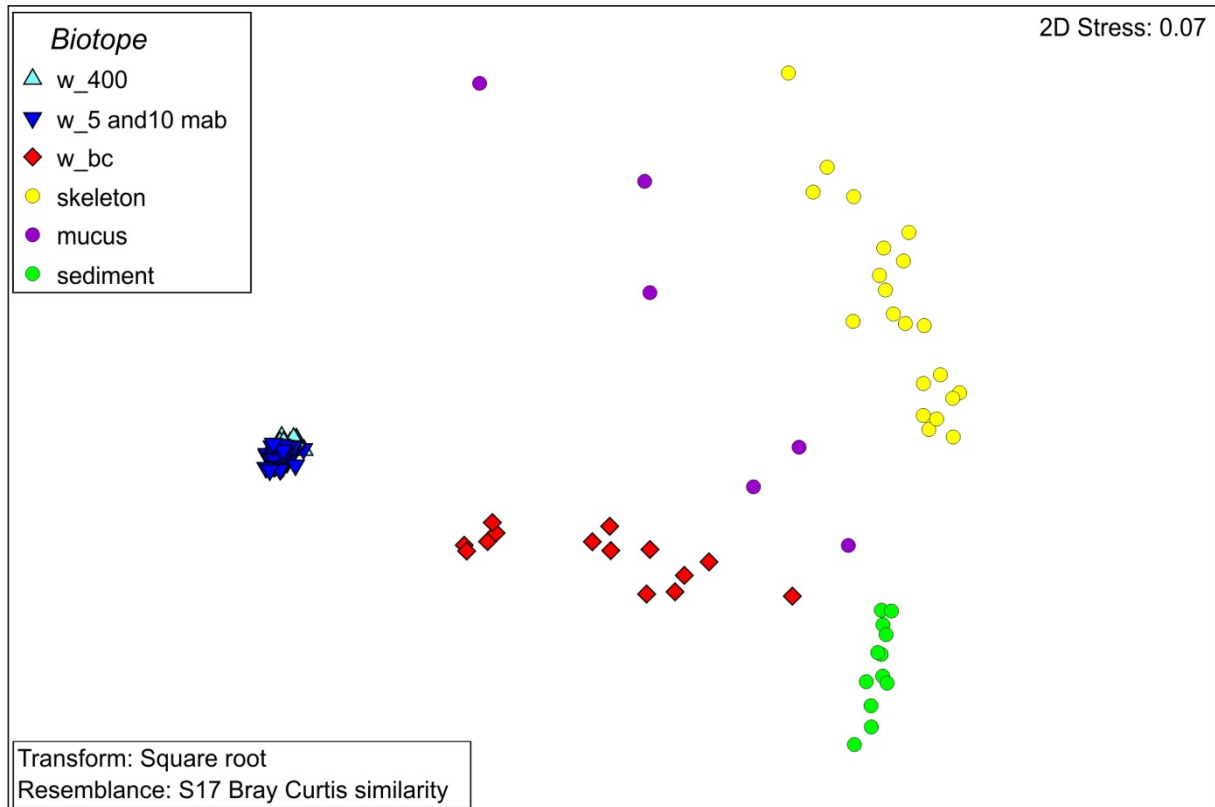
Sample group (#strong indicators)	Indicator	A	B	stat	p.value	Reads avg % in sample group
w_CTD (4/38)	uncl. SAR11 clade Deep 1	0.8833	1.0000	0.940	0.0001	2.61
	Rhodospirillaceae AEGEAN-169 marine group	0.8796	1.0000	0.938	0.0001	2.20
	uncl. Verrucomicrobia Arctic97B-4 marine group	0.8751	1.0000	0.935	0.0001	0.45
	uncl. Thermoplasmatales Marine Group III	0.8721	1.0000	0.934	0.0001	1.00
	uncl. Oceanospirillales ZD0405	0.8361	1.0000	0.914	0.0001	2.85
w_bc (8/13)	uncl. Dehalococcoidia vadinBA26	0.9437	1.0000	0.971	0.0001	0.36
	uncultured Oceanospirillaceae	0.9460	0.8571	0.900	0.0001	0.05
	uncl. Dehalococcoidia GIF3	1.0000	0.7143	0.845	0.0001	0.27
	uncl. BHI80-139	0.8931	0.7857	0.838	0.0001	0.07
	uncl. Dehalococcoidia Sh765B-AG-111	1.0000	0.6429	0.802	0.0001	0.09
	Sphingobacteriales KD1- 131	0.8881	0.7143	0.796	0.0001	0.09
	Thaumarchaeota Group C3	1.0000	0.5714	0.756	0.0001	0.03
	Brocadiaceae W4	0.9982	0.5000	0.706	0.0001	0.83
sediment (0/3)	Phycisphaerae C86	0.6982	1.0000	0.836	0.0001	0.25
	uncl. Chloroflexi JG30-KF- CM66	0.5118	1.0000	0.715	0.0001	0.56
	uncl. Rhodospirillales AT- s3-44	0.3669	1.0000	0.606	0.0001	0.32
skeleton (0/12)	uncul. Caldilineaceae	0.7979	1.0000	0.893	0.0001	0.71
	<i>Granulosicoccus</i>	0.7513	1.0000	0.867	0.0001	1.87
	<i>Profundibacterium</i>	0.7602	0.9524	0.851	0.0001	0.22

mucus (12/12)	uncl. Oceanospirillales G02-CR02-full	0.9982	1.0000	0.999	0.0001	0.36
	<i>Acinetobacter</i>	0.9872	1.0000	0.994	0.0001	9.11
	uncult. Helicobacteraceae	0.9699	1.0000	0.985	0.0001	0.48
	uncl. Oceanospirillales BPS-CK174	0.9651	1.0000	0.982	0.0001	0.29
	Alteromonadaceae BD1-7 clade	0.9636	1.0000	0.982	0.0001	22.00
	<i>Corynebacterium</i>	0.9259	1.0000	0.962	0.0001	0.11
	<i>Staphylococcus</i>	0.9169	1.0000	0.958	0.0001	0.06
	<i>Sphingomonas</i>	0.9000	1.0000	0.949	0.0001	0.15
	<i>Enhydrobacter</i>	0.9963	0.8333	0.911	0.0001	0.17
	<i>Methylobacterium</i>	0.9705	0.8333	0.899	0.0001	0.24
	<i>Tumebacillus</i>	0.9106	0.8333	0.871	0.0001	0.13
	<i>Micrococcus</i>	0.9773	0.5000	0.699	0.0001	0.06

712

713

714 **S.I. Figure 1.** MDS plot of microbial community on OTU level of the individual samples showing  
715 clustering according to sample category: overlaying water (400 m and 5 and 10 mab), near-bottom  
716 water (w\_bc), sediment, skeleton and mucus.  
717

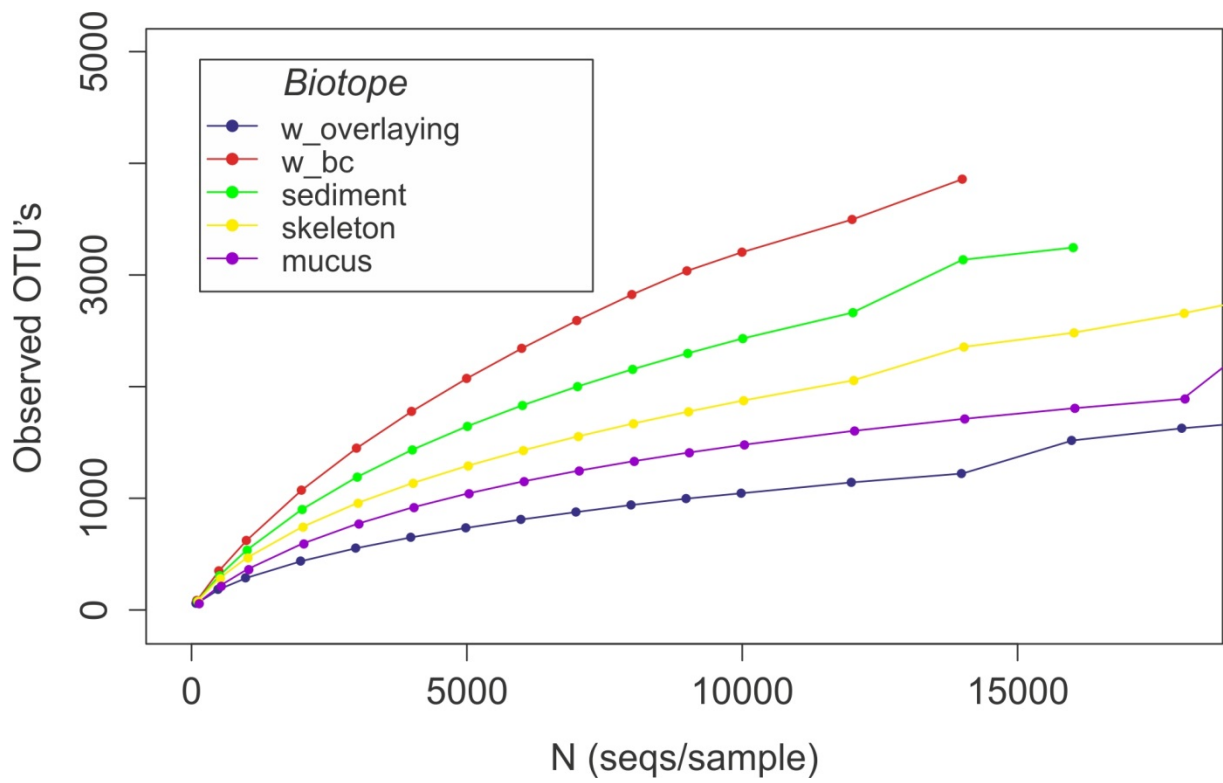


718

719



720 **S.I. Figure 2.** Rarefaction curves of OTU's plotted against reads per sample.



721

722

723